HHS Public Access

Author manuscript

J Mater Chem B Mater Biol Med. Author manuscript; available in PMC 2016 July 14.

Published in final edited form as:

J Mater Chem B Mater Biol Med. 2015 July 14; 3(26): 5361–5376. doi:10.1039/C5TB00353A.

A biphasic scaffold based on silk and bioactive ceramic with stratified properties for osteochondral tissue regeneration

Jiao Jiao Li[1], **Kyungsook Kim**[2], **Seyed-Iman Roohani-Esfahani**[1], **Jin Guo**[2], **David L. Kaplan**[2], and **Hala Zreiqat**[1,*]

[1]Biomaterials and Tissue Engineering Research Unit, School of AMME, University of Sydney, Sydney, NSW 2006, Australia

[2]Department of Biomedical Engineering, Tufts University, Medford, MA 02155, USA

Abstract

Significant clinical challenges encountered in the effective long-term treatment of osteochondral defects have inspired advancements in scaffold-based tissue engineering techniques to aid repair and regeneration. This study reports the development of a biphasic scaffold produced via a rational combination of silk fibroin and bioactive ceramic with stratified properties to satisfy the complex and diverse regenerative requirements of osteochondral tissue. Structural examination showed that the biphasic scaffold contained two phases with different pore morphologies to match the cartilage and bone segments of osteochondral tissue, which were joined at a continuous interface. Mechanical assessment showed that the two phases of the biphasic scaffold imitated the load-bearing behaviour of native osteochondral tissue and matched its compressive properties. *In vitro* testing showed that different compositions in the two phases of the biphasic scaffold could direct the preferential differentiation of human mesenchymal stem cells towards the chondrogenic or osteogenic lineage. By featuring simple and reproducible fabrication and a well-integrated interface, the biphasic scaffold strategy established in this study circumvented the common problems experienced with integrated scaffold designs and could provide an effective approach for the regeneration of osteochondral tissue.

Graphical Abstract

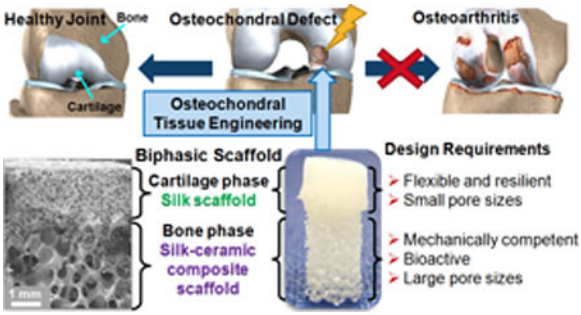

*Corresponding author: Prof. Hala Zreiqat, School of AMME, University of Sydney, Sydney, NSW 2006, Australia, Phone: +61 2 93512392, Fax: +61 2 93517060, hala.zreiqat@sydney.edu.au.

Keywords

osteochondral defects; biphasic scaffold; silk fibroin; bioactive ceramic; tissue engineering

1. Introduction

The management and reconstruction of damaged or diseased osteochondral tissue at skeletal joints have remained a significant orthopaedic challenge. Existing clinical treatments may be effective in alleviating pain and morbidity in the short term, but rarely achieve full restoration of functional osteochondral tissue in the long term.[1] Reparative techniques such as microfracture often result in the formation of fibrocartilage that lacks clinical durability,[2] and the success of restorative techniques is limited by the availability of donor tissue for osteochondral grafts[3] or graft delamination, insufficient cartilage regeneration and the lack of long-term results for the generations of autologous chondrocyte implantation (ACI).[4] The inability to achieve adequate repair over time can cause osteochondral defects to expand and contribute to degenerative joint changes, which eventually lead to the progression of osteoarthritis and result in severe pain, joint deformity and loss of joint motion.[5] The unique and complex nature of osteochondral tissue poses significant challenges to satisfactory repair and regeneration, due to their stratified structure involving multiple tissue segments including articular cartilage, subchondral bone and interfacial tissues.[6] Current treatment modalities are still struggling to tackle the different compositional, structural, mechanical and biochemical requirements of each tissue component in the osteochondral unit. Driven by the growing unmet clinical need to develop more effective therapies, scaffold-based osteochondral tissue engineering strategies have emerged in recent years with the aim of arriving at a viable product that can address the diverse regenerative requirements of osteochondral tissue.[7–11]

Many different osteochondral scaffold strategies have evolved and can be broadly classified into several categories: monophasic scaffolds,[12–19] scaffolds for the bone part with cells for the cartilage part,[20–23] assembled scaffolds with individual scaffolds for cartilage and bone,[24–30] homogeneous scaffolds with different cell populations for cartilage and bone[31–33] or a continuous gradient of bioactive molecules,[34–37] and single scaffolds with integrated phases.[38–49] These scaffolding approaches each have their own advantages and disadvantages which govern their effectiveness, but the efficient translation of individual strategies is additionally restricted by practical requirements including ease and reproducibility of fabrication, choice of materials which are already approved (or likely to obtain approval) for human use, sterilisability, and the preference for products which can be used independently without the incorporation of cells and/or bioactive molecules.[50] The difficulty in developing a scaffold that simultaneously satisfies the structural, mechanical and biological requirements of osteochondral regeneration alongside stringent regulatory requirements explains the scarcity of commercialised scaffold-only products for the treatment of osteochondral defects and their limited[51–54] or unsatisfactory[55–57] long-term outcomes.

Assessing the different types of scaffold-based tissue engineering strategies against the diverse sets of requirements for the regeneration of osteochondral tissue, a single scaffold with integrated phases stands out as an effective and practical approach. This type of scaffold design features two or more phases potentially with unique properties in each phase to match the different regenerative requirements in each segment of the osteochondral unit.[50] The phases are integrated during fabrication to produce a continuous transition in interfacial properties.[11] A heterogeneous structure is therefore possible with a wide range of material choices and without the formation of a sharp interface which is biologically undesirable.[10] Furthermore, because the complete scaffold is formed prior to any *in vitro* or *in vivo* interaction, this strategy offers the attractive possibility of being adopted for translational use without necessitating the inclusion of cells and/or bioactive molecules. A scaffold design featuring integrated phases composed of common bioactive materials therefore has great potential in becoming a viable product for the effective treatment of osteochondral defects. However, some common challenges experienced with similar designs must be considered and addressed, including potentially poor integration between phases, complex and/or impractical processing methods, and lack of reproducibility.[50]

The purpose of this study was to design, optimise and characterise an osteochondral scaffold with integrated phases via a rational combination of bioactive materials. The design concept involved a scaffold with two integrated phases overlapping at the interface. The two phases were respectively targeted for the regeneration of articular cartilage and subchondral bone in the osteochondral unit, and the material choices of each phase were determined by the structural, mechanical and biological requirements of the two tissues (Fig. 1). Simple and reproducible fabrication methods and good integration between phases were factors which guided the optimisation of the design, in light of the common challenges experienced with other integrated scaffold strategies. A biphasic scaffold design was established with a silk protein scaffold constituting the cartilage phase and a silk-coated strontium-hardystonite-gahnite ceramic scaffold (SHG-silk) constituting the bone phase. Fabrication processes were optimised to produce the two phases of the biphasic scaffold with unique and stratified properties together with a well-integrated interface. Systematic investigations were performed to evaluate the physical and mechanical properties of the biphasic scaffold, as well as its *in vitro* behaviour when cultured in the presence of human mesenchymal stem cells (hMSCs). The results indicated that the stratified properties of the biphasic scaffold could meet the regenerative requirements of osteochondral tissue, and might be useful for the identification of design parameters in the development of biomimetic osteochondral scaffolds. Stratified scaffolds featuring an integrated design, such as the biphasic scaffold developed in this study, could contribute to the new paradigm of using scaffold-only tissue engineering strategies to resolve the clinical challenges encountered in the management and reconstruction of osteochondral defects.

2. Experimental

Silk fibroin aqueous solution prepared from *Bombyx mori* cocoons via a previously described method[58] was used for all subsequent experiments.

2.1 Preparation of strontium-hardystonite-gahnite (SHG) ceramic scaffolds

SHG ceramic scaffolds were prepared to desired dimensions for use in subsequent experiments. Sr-$Ca_2ZnSi_2O_7$ powder was prepared by the sol-gel method (reagents from Sigma-Aldrich, St. Louis, MO, USA) as previously described,[59] to which aluminum oxide (Al_2O_3) powder (15 wt%) was added. The powders were mixed and ground using a planetary ball mill (Retsch PM 400, Haan, Germany) for 2 hours at 150rpm to give particles of 10–20μm size for scaffold preparation. The polymer sponge method was used for scaffold fabrication. Fully reticulated polyurethane foam (The Foam Booth, Sydney, Australia) was cut to appropriate dimensions and used as sacrificial templates for scaffold replication. The ceramic slurry was prepared by adding the ceramic powder to 0.01 M polyvinyl alcohol (PVA) binder solution to make a 30 wt% suspension. Foam templates were immersed in the ceramic slurry and compressed gently a few times to facilitate slurry penetration, and excess slurry was squeezed out. After drying, SHG ceramic scaffolds were produced by sintering the ceramic-coated foams in air in an electric furnace using a five-stage schedule: (i) heating from 25°C to 400°C at a heating rate of 1°C min^{-1}, (ii) holding the temperature at 400°C for 1 hour, (iii) heating from 400°C to 1250°C at 2°C min^{-1}, (iv) holding at 1200°C for 3 hours, and (v) cooling to 25°C at a cooling rate of 5°C min^{-1}.

2.2 Preparation of SHG-silk scaffolds (bone phase)

SHG-silk scaffolds were prepared for use in subsequent experiments by coating SHG ceramic scaffolds with a single silk layer using an aqueous silk fibroin solution with a concentration of *ca*. 8 wt%. The coating process involved immersing the ceramic scaffold in silk solution and pipetting the solution through the scaffold to ensure uniform infiltration. Excess silk solution was removed from the scaffold with tissues before vacuum drying at 80°C for 30 min. The silk coating was stabilised by immersing the coated scaffold in methanol for 5 min to induce β-sheet formation, followed by vacuum drying at 80°C for 10 min.

2.3 Preparation of silk scaffolds (cartilage phase) for characterisation

Silk scaffolds were prepared via phase separation induced by freezing aqueous silk fibroin solution in the presence of a small amount of organic solvent, by adaption of a previously described method.[60] Specifically, aqueous silk fibroin solution and diluted methanol solution were homogeneously mixed via pipetting to final concentrations of 4 wt% silk fibroin and 2 vol% methanol. The mixture was dispensed to cylindrical moulds of appropriate diameter (corresponding to the desired diameter of silk scaffolds) and immediately frozen at −20°C for at least 8 hours. Porous silk scaffolds were formed after thawing at room temperature and traces of methanol were removed by washing in distilled water. The washes were performed by immersing the silk scaffolds in water at a ratio of *ca*. 100mL water per $1cm^3$ scaffold. The scaffolds were gently rocked for at least 6 hours during each wash and the washing process was repeated at least 6 times. The resulting silk scaffolds were trimmed in length if necessary and stored in distilled water at 4°C for use in subsequent experiments.

2.4 Preparation of biphasic scaffolds

Biphasic scaffolds were prepared by mounting the SHG-silk scaffold inside the mixture of silk and methanol prior to silk scaffold formation (Supplementary Fig. 1). Specifically for the preparation of each biphasic scaffold, a homogeneous mixture of silk and methanol (concentrations as specified in Section 2.3) was dispensed to a cylindrical mould of appropriate diameter and a SHG-silk scaffold with diameter just less than that of the mould was inserted into the mixture. The position of the SHG-silk scaffold was adjusted and secured with paraffin film such that approximately one-third of its length was immersed in the silk mixture to form the interface region of the biphasic scaffold. The silk mixture with the mounted SHG-silk scaffold was immediately frozen at −20°C for at least 8 hours. Biphasic scaffolds with a cartilage phase consisting of a silk scaffold attached to a bone phase consisting of a SHG-silk scaffold was formed after thawing at room temperature, and traces of methanol in the silk scaffold were removed by washing the biphasic scaffold in distilled water as described in Section 2.3. The resulting biphasic scaffolds were adjusted in length by trimming the silk scaffold if necessary and stored in distilled water at 4°C for use in subsequent experiments.

2.5 Physical properties of the biphasic scaffold

The scaffolds were freeze-dried using a FreeZone 4.5L Benchtop Freeze Dry System −105°C (Labconco, Kansas City, MO, USA) for 2 days. Freeze-dried scaffolds were fractured in liquid nitrogen using a razor blade and sputter coated with gold. Pore morphology and microstructure of the scaffolds were examined via field emission scanning electron microscopy (FE-SEM) using Zeiss Ultra (Carl Zeiss, Oberkochen, Germany).

2.6 Mechanical properties of the biphasic scaffold

Mechanical properties of the scaffolds were determined on five independent samples for each test. Tests conducted on the biphasic scaffold were: 1) tension testing on hydrated modified biphasic scaffolds (where the SHG-silk scaffold had silk scaffolds attached to both ends to allow clamping, 8.5mm diameter by 65mm gauge length) to determine interfacial bonding strength, and 2) compression testing on hydrated biphasic scaffolds (7.5mm diameter by 21mm height including 7mm silk scaffold height). Other tests conducted were: 1) tension testing on the silk scaffold as an independent construct (8.5mm diameter by 8mm gauge length), and 2) compression testing on the silk scaffold and SHG-silk scaffold as independent constructs (7.5mm diameter by 7mm height for both groups). All samples were tested in air using a computer-controlled Instron 5567 (Buckinghamshire, UK) testing frame equipped with a 100N capacity load cell for tension testing or a 1kN capacity load cell for compression testing. All tests were conducted using a displacement control mode with crosshead displacement rate of 2mm min^{-1}. For the biphasic scaffold in tension, the interfacial bonding strength was measured at the maximum peak on the stress-strain curve (point of breakage). For the silk scaffold in tension, the maximum peak on the stress-strain curve was used to determine the ultimate tensile strength and strain at failure, and the elastic modulus was calculated as the slope of the curve in the initial linear region. For the biphasic scaffold in compression, the compressive strength and modulus of the silk scaffold and SHG-silk scaffold were determined separately based on the section of the stress-strain curve

corresponding to each phase. For the silk scaffold section, the compressive strength was measured at the point where a line drawn parallel to the initial linear region of the stress-strain curve starting at 1% compressive strain crossed the curve, according to a previously described method.[58] The compressive modulus was calculated as the slope of the curve in the initial linear region. For the SHG-silk scaffold section, the highest peak in the stress-strain curve within the first millimeter of compressive extension was used to determine the compressive strength and modulus. Compressive strength was measured as the maximum stress at the top of the peak, and the compressive modulus was calculated as the slope of the curve leading up to the peak. Compression testing was performed on the silk scaffold and SHG-silk scaffold to obtain stress-strain curves for comparison with the biphasic scaffold.

2.7 Cell culture

All reagents were purchased from Life Technologies (Grand Island, NY, USA) unless otherwise stated. hMSCs were extracted from a single donor from commercially obtained fresh human bone marrow aspirate (Lonza, Walkersville, MD, USA). Aspirate donors were male, under 25 years of age and free of HIV, hepatitis B and hepatitis C. The aspirate was diluted 10-fold with expansion medium consisting of Dulbecco's Modified Eagle Medium (DMEM) supplemented with 10% fetal bovine serum (FBS), antibiotics-antimycotics (100U mL^{-1} penicillin, 100μg mL^{-1} streptomycin, 0.25μg mL^{-1} fungizone), 0.1mM non-essential amino acids, and 1ng mL^{-1} basic fibroblast growth factor (bFGF). The diluted aspirate was plated in T-185 flasks at an average seeding density of 3.5×10^5 bone marrow mononuclear cells per cm^2. Cells were rocked daily to re-suspend non-adherent cells and were cultured for 14 days at 37°C in 5% CO_2 (with 20mL of fresh medium replenished twice per week), after which the non-adherent cells (haematopoietic cells) were removed and adherent cells (hMSCs) were kept in expansion medium to reach confluence. No sorting of the cells was performed and cells were tested for chondrogenic, osteogenic and adipogenic differentiation by monolayer and micromass culture (Supplementary Fig. 2).

Biphasic scaffolds used for the *in vitro* experiments had dimensions of 6mm diameter by 10mm height (including 5mm silk scaffold height), while silk scaffolds, SHG ceramic scaffolds and SHG-silk scaffolds included for comparison as independent constructs had dimensions of 6mm diameter by 5mm height. Scaffolds were sterilised by autoclaving, placed in 12-well plates, incubated overnight in expansion medium and aspirated prior to cell seeding. All hMSCs used for seeding were at passage 4. After the cells reached 80–90% confluence, they were trypsinised and subsequently suspended in expansion medium. hMSCs were seeded by dropping the cell suspension homogeneously onto the scaffolds at a seeding density of 1×10^6 cells per scaffold. The seeded scaffolds were incubated for 2 hours at 37°C to allow cell attachment, after which 1.5mL of expansion medium was added to each well. After 24 hours, the expansion medium was replaced with 1.5mL of differentiation medium. Cultures were maintained at 37°C in 5% CO_2, and 1.5mL of differentiation medium was replaced completely every 3 days. For the evaluation of cell attachment, scaffolds were collected after 2 and 24 hours of culture in expansion medium. For histological and immunofluorescence staining, scaffolds were collected after 21 days of culture in chondrogenic medium. For gene expression analysis, scaffolds were collected after 4, 14 and 21 days of culture in both chondrogenic and osteogenic media. Chondrogenic

medium consisted of DMEM supplemented with antibiotics-antimycotics (100U mL^{-1} penicillin, 100μg mL^{-1} streptomycin, 0.25μg mL^{-1} fungizone), ITS^{+1} (10μg mL^{-1} insulin, 5.5μg mL^{-1} transferrin, 5ng mL^{-1} selenium, 0.5mg mL^{-1} bovine serum albumin, 4.7μg mL^{-1} linoleic acid; Sigma-Aldrich), 0.1mM ascorbic acid 2-phosphate (Sigma-Aldrich), 1.25 mg mL^{-1} human serum albumin (Sigma-Aldrich), 100nM dexamethasone (Sigma-Aldrich), and 10ng mL^{-1} TGF-β3 (PeproTech, Rocky Hill, NJ, USA). Osteogenic medium consisted of α-minimum essential medium (α-MEM) supplemented with 10% FBS, antibiotics-antimycotics (100U mL^{-1} penicillin, 100μg mL^{-1} streptomycin, 0.25μg mL^{-1} fungizone), 0.1mM non-essential amino acids, 10mM β-glycerol-2-phosphate (Sigma-Aldrich), 100nM dexamethasone (Sigma-Aldrich), and 0.05mM L-ascorbic acid (Sigma-Aldrich).

2.8 Cell attachment

Cultured scaffolds were analysed for the attachment of hMSCs. At each time point, scaffolds were harvested and fixed in 4% PBS buffered paraformaldehyde for at least 24 hours. The scaffolds were rinsed in PBS and dehydrated through graded ethanol (50%, 70%, 95% and 100%), dried in hexamethyldisilizane for 3 min and then desiccated overnight. The scaffolds were sputter coated with gold prior to SEM examination using Zeiss Ultra (Carl Zeiss).

2.9 Histology and immunofluorescence

Scaffolds cultured in chondrogenic medium were harvested for histological and immunofluorescence staining and fixed in 4% PBS buffered paraformaldehyde for at least 24 hours. The scaffolds were dehydrated through graded ethanol (70%, 80%, 90%, 95% and 100%), embedded in paraffin and sectioned at 8μm thickness. For histological localisation of sulfated glycosaminoglycan (GAG) distribution within the scaffolds, sections were deparaffinised and rehydrated to distilled water, followed by staining with 0.1% Alcian blue in 0.4M $MgCl_2$ and 0.025M sodium acetate (pH 5.6) and counterstaining with nuclear fast red. For immunofluorescence staining of collagen type II deposition within the scaffolds, non-specific binding sites were first blocked with 10% goat serum (Vector laboratories, Burlingame, CA, USA) for 30 min. The sections were incubated with rabbit anti-collagen II antibody (1:100 dilution; Abcam, Cambridge, MA, USA) for 12 hours at 4°C, followed by staining with Alexa Fluor® 594 goat anti-rabbit IgG antibody (Life Technologies) for 1 hour. The nuclei were stained with Prolong® Antifade Reagents (Life Technologies). The sections were mounted to slides and imaged on a Leica DM IL optical microscope (Wetzlar, Germany) equipped with a Leica DFC295FX camera for Alcian blue images and a Leica DFC340FX camera for immunofluorescence images.

2.10 Gene expression

Quantitative real time reverse transcription polymerase chain reaction (qRT-PCR) was used to evaluate chondrogenic and osteogenic gene expression of hMSCs on the cultured scaffolds. Samples of cells at day 0 just prior to seeding were collected in Trizol and stored at −80°C. At each time point, scaffolds were rinsed in PBS and stored in Trizol at −80°C. For analysis, the scaffolds were thawed and chopped using microscissors. RNA was isolated using the single step acid-phenol guanidinium method, and purified using the PureLink® RNA Mini Kit (Life Technologies) according to the manufacturer's instructions. cDNA was

synthesised from 1μg total RNA by reverse transcription using the High Capacity cDNA Archive Kit (Applied Biosystems, Foster City, CA, USA) according to the manufacturer's instructions. Primer sequences from TaqMan® Gene Expression Assays (Life Technologies) were used for the housekeeping gene glyceraldehyde 3-phosphate dehydrogenase (GAPDH, Hs99999905_m1), the chondrogenic genes Sox-9 (SOX9, Hs01001343_g1), aggrecan (ACAN, Hs00153936_m1), collagen type II (COL2A1, Hs00264051_m1), and collagen type X (COL10A1, Hs00166657_m1), and the osteogenic genes Runx2 (RUNX2, Hs00231692_m1), collagen type I (COL1A1, Hs00164004_m1), alkaline phosphatase (ALPL, Hs01029144_m1), and bone sialoprotein (IBSP, Hs00173720_m1). Expression levels of all genes were quantified using an ABI Prism 7000 Sequence Detection System (Applied Biosystems) and normalised to GAPDH using the comparative Ct ($2^{-\Delta\Delta Ct}$) method.

2.11 Statistical analysis

Data for all experiments were obtained from four independent samples unless otherwise specified. All data were expressed as mean ± standard deviation and analysed using one-way ANOVA. Differences were considered as statistically significant for $p < 0.05$.

3. Results and discussion

3.1 Optimisation of biphasic scaffold design and fabrication

The design of the biphasic scaffold was established from the combination of a flexible and resilient silk scaffold for the cartilage phase and a mechanically strong and bioactive SHG-silk scaffold for the bone phase. Scaffold selection for the bone phase was based on emerging evidence that the subchondral bone could mediate chondrogenesis in an osteochondral environment[61] and play a critical role in the outcome of cartilage repair.[62] It was therefore desirable to choose a scaffold that could facilitate adequate restoration of the subchondral bone in a load-bearing environment, which not only mimicked the structural and mechanical characteristics of cancellous bone but also possessed bioactivity and the ability to promote osteogenesis *in vivo*. The strontium-hardystonite-gahnite (SHG) ceramic scaffold which we have previously developed was an exact match for these criteria. Its unique properties originate from a microstructure featuring solid high-density struts and composition containing the bioactive ions Sr, Ca, Zn and Si, which contribute to its excellent osteogenic potential both *in vitro* and *in vivo* (rabbit segmental defect model).[59] The SHG ceramic scaffold was coated with a single layer of silk fibroin to form the SHG-silk scaffold of the bone phase. The purpose of the silk coating was to facilitate adequate integration with the cartilage phase and allow control over size of the interface region, with the added benefit of enhancing the toughness of the ceramic scaffold by reducing the chance of crack propagation under load.[63] Scaffold selection for the cartilage phase depended on the choice of a polymeric material to imitate the nature of the cartilaginous matrix, coupled with the practical requirements of processing simplicity and ability to be integrated with the bone phase. Natural polymers were considered as they often mimic the extracellular matrix (ECM) and present structural and biochemical signals which are desirable for tissue regeneration, and can also degrade *in vivo* without the formation of potentially harmful by-products as often encountered by synthetic polymers.[7] Of these, silk fibroin was the best candidate material as it did not face the common problems of natural polymers including

low mechanical strength and rapid or variable degradation *in vivo*.[64] A silk scaffold was therefore chosen for the cartilage phase, which was backed by its ease of processing via versatile fabrication methods,[65] experimental evidence for its ability to form cartilaginous constructs *in vitro*,[66–71] and its long-term stability and biocompatibility *in vivo*.[72]

Fabrication processes were optimised in order to realise the design of the biphasic scaffold with desirable characteristics for osteochondral regeneration while ensuring a well-integrated interface. The polymer sponge method was used to fabricate the SHG ceramic scaffold as it could easily produce a highly porous and interconnected construct resembling cancellous bone while offering control over the pore structure.[73] Phase separation induced by freezing aqueous silk fibroin solution in the presence of a small amount of organic solvent[60] was the method used to fabricate the silk scaffold as it allowed reliable integration between the cartilage and bone phases, and scaffold characteristics favourable for cartilage regeneration were produced after optimisation of this method in terms of choice of solvent, concentration of solvent, concentration of silk fibroin solution, choice of freezing temperature, and choice of freezing duration (data not shown). Silk coating on the SHG ceramic scaffold was necessary for the controlled formation of the biphasic scaffold with well-integrated and distinct phases. Biphasic scaffold formation required the bone phase scaffold to be partially immersed in the mixture of silk and solvent used to form the cartilage phase prior to and during freezing. Without the silk coating, a large portion of the mixture was immediately absorbed into the SHG ceramic scaffold due to its hydrophilic surface, producing a biphasic scaffold with weakly integrated phases and offering little control over the size of the interface region. In contrast, the SHG-silk scaffold had a hydrophobic surface[65,74] due to the presence of the silk coating, which prevented absorption of the mixture beyond the interface region. Optimisation of the fabrication variables hence allowed the biphasic scaffold to be produced via a simple, reproducible and customisable procedure (Fig. 2A). By adjusting the size of the mould used to hold the silk mixture, the size of the polymer sponge template used to make the SHG-silk scaffold, and the amount of overlap between the two phases, biphasic scaffolds with customised dimensions to suit osteochondral regeneration at different sites could be easily and reproducibly prepared with control over the proportions of the two phases and the interface region (Fig. 2B).

3.2 Morphology and microstructure of the biphasic scaffold

SEM examination showed that the biphasic scaffold contained two phases with distinctly different pore structures which were integrated at an overlapping interface (Fig. 3A). The silk scaffold constituted the cartilage phase in the top portion of the biphasic scaffold (Fig. 3B), and the SHG-silk scaffold constituted the bone phase in the bottom portion (Fig. 3D). The cartilage and bone phases were integrated at a coherent interface which displayed a transitional blend of the structural properties belonging to each of the two phases (Fig. 3C). Closer examination showed that the silk scaffold of the cartilage phase had small pore sizes of 100–120μm, and the pores were highly interconnected as the pore walls contained many smaller pores of 20–40μm diameter (Fig. 3E). The microscopic morphology of the silk scaffold was similar to that observed in other studies which produced porous silk matrices via phase separation.[60,75,76] In contrast, the SHG-silk scaffold of the bone phase had large pore sizes of 400–500μm accompanied by high porosity and interconnectivity (Fig. 3G). The

scaffold struts were solid and continuous with no obvious defects and few micropores. This was due to the unique microstructure of the SHG ceramic, which accounted for its remarkable mechanical properties matching those of cancellous bone.[59] The interface region consisted of a silk matrix filling the open pores of the SHG-silk backbone with coherent bonding between the two structures (Fig. 3F). This blending of the cartilage and bone phases resulted in the formation of a continuous interface with smooth transition between the phases, which could contribute to interfacial bonding strength and promote biological interactions in the interface region. The stratified structure of the biphasic scaffold was made possible by the thin silk coating layer on the SHG-silk scaffold (Fig. 3G, **inset**) as discussed in Section 3.1, which allowed the formation of distinct cartilage and bone phases while offering control over the size of the interface region.

The pore sizes of a scaffold are known to have profound effects in directing the differentiation of mesenchymal progenitor cells towards the chondrocyte or osteoblast lineage.[77,78] Smaller pores introduce hypoxic conditions with low oxygen tension, which tend to limit vascular invasion and result in chondrogenesis. In contrast, larger pores promote rapid vascularisation due to high oxygen tension and lead to direct osteogenesis.[79] The influence of pore size on the formation of cartilage or bone tissue was experimentally established in studies which showed that scaffolds of the same composition induced chondrogenesis in the presence of smaller pore sizes (80–120μm) and osteogenesis in the presence of larger pore sizes (>300μm) after subcutaneous implantation into rats.[80–82] The formation of cartilage or bone tissue was related to different scaffold geometries which restricted or enhanced vascularisation. In the biphasic scaffold, small pores in the cartilage phase could be expected to promote chondrogenesis by limiting vascularisation, while large pores in the bone phase could be expected to promote osteogenesis by enhancing vascularisation. High pore interconnectivity in both phases would facilitate adequate cell penetration and the exchange of nutrients and waste products.

The microscopic morphology of the biphasic scaffold presented unique features which were favourable for osteochondral regeneration. The integrated phases of the biphasic scaffold displayed heterogeneous structural characteristics which were defined by distinctly different pore morphologies in the cartilage and bone phases to suit the regenerative requirements of each osteochondral segment. The two phases were well-integrated at a continuous interface to form the coherent structure of the biphasic scaffold, via a simple fabrication method that allowed control over the size of the interface region. The realisation of this biphasic scaffold design therefore circumvented many of the common issues encountered with other integrated scaffold designs featuring stratified layers with heterogeneous properties, including the lack of smooth transition between phases,[38,39,41,42,45,47,49] lack of control over the size of the interface region,[44,48] and complicated or tedious fabrication methods.[42,43]

3.3 Mechanical properties of the biphasic scaffold

The silk scaffold was first tested independently in tension and exhibited highly elastic behaviour which was desirable for the cartilage phase of the biphasic scaffold, with measured values of 45 ± 6 kPa for ultimate tensile strength, 39 ± 9 kPa for elastic modulus, and 91 ± 13% for strain at failure. The significant strain at failure value indicated that the

silk scaffold could stretch to approximately twice its original length before breakage, which greatly exceeded the values observed for collagen fibres[83] and synthetic polymers including polyglycolic acid, polylactic acids and polycaprolactone.[84] The silk scaffold also compared well with other silk-based scaffolds formed via phase separation in terms of ultimate tensile strength[60,85] and elastic modulus.[85]

Interfacial bonding strength between the two phases of the biphasic scaffold was then determined by testing modified biphasic scaffolds in tension, which consisted of long silk scaffolds attached to both ends of the SHG-silk scaffold (Fig. 4A). During testing, a portion of the silk scaffold at each end of the modified biphasic scaffold was clamped and the initial gauge length was set such that the silk scaffolds at both ends were fully extended but not stretched (Fig. 4B). As the modified biphasic scaffold was pulled in tension, the interface between the silk scaffold and SHG-silk scaffold at either end initially exhibited elastic deformation until the yield point was reached (Fig. 4E, **orange arrow**), which was followed by plastic deformation until the breaking point (Fig. 4E, **red arrow**). After this, continuous deformation led to gradual dissociation of the interface (Fig. 4C) until complete breakage occurred (Fig. 4D). For all samples, breakage occurred in either the top or bottom interface region of the modified biphasic scaffold. The interface behaviour of the biphasic scaffold followed the mechanical profile of cellular solids in tension.[86] The interfacial bonding strength was measured to be 29 ± 4 kPa between the two phases of the biphasic scaffold, which was approximately 65% of the ultimate tensile strength of the silk scaffold and also compared well with the failure strengths obtained for other integrated scaffold designs.[39,87] The simple method used for biphasic scaffold fabrication could therefore achieve adequate bonding between the cartilage and bone phases, with sufficient strength in the interface region to resist shear stresses in the physiological joint environment considering that the majority of biomechanical loading on articular cartilage occurred in compression.[88]

To evaluate its relevance for potential use in a load-bearing osteochondral environment, the mechanical behaviour of the biphasic scaffold was determined in compression. The biphasic scaffold used for testing comprised two integrated phases of approximately equal proportions (Fig. 5A). As the biphasic scaffold was subjected to uniaxial compression, the silk scaffold initially underwent elastic deformation (Fig. 5B) and samples retrieved at this stage could easily recover their original shape. As the test progressed, plastic deformation was observed in the silk scaffold (Fig. 5C) and samples retrieved at this stage exhibited partial shape recovery with some permanent deformations. Further compressive extension resulted in compaction of the silk scaffold and load transfer to the underlying SHG-silk scaffold (Fig. 5D). Samples retrieved at the end of compression testing consisted of a flattened silk scaffold which remained well-integrated to the SHG-silk scaffold with no signs of delamination between phases, and little visible deformation was noted in the SHG-silk scaffold (Fig. 5E). The biphasic scaffold therefore maintained its structural integrity and adequate bonding between phases even after being tested to failure under high compressive stresses that would not be encountered in physiological conditions. The mechanical behaviour of the biphasic scaffold in compression was reflected by its stress-strain curve (Fig. 5F). The first section of the curve was smooth and corresponded to the compressive response of the silk scaffold, while the second section displayed the characteristic response

of ceramic-based scaffolds in compression and corresponded to the SHG-silk scaffold. The initial linear region of the curve indicated elastic deformation of the silk scaffold, followed by a plateau region of plastic deformation during silk scaffold yielding, before densification of the silk scaffold and transfer of the compressive load to the SHG-silk scaffold. The SHG-silk scaffold exhibited impressive load-bearing behaviour as evidenced by the large area under the corresponding section of the stress-strain curve, indicating that a large amount of energy was absorbed before scaffold deformation and eventual failure.

Compressive properties of the biphasic scaffold were determined and values for each of the two phases are presented in Table 1. The compressive modulus of native osteochondral tissue follows a gradient that ranges from 0.079MPa in the superficial layer of articular cartilage to 5.7GPa in the subchondral bone.[89] The biphasic scaffold possessed stratified compressive properties due to the different mechanical behaviour of its two phases, which imitated the mechanical transition in the different segments of osteochondral tissue and also matched the stiffness of each segment. Furthermore, consistent with its role as the load-bearing phase of the biphasic scaffold, the SHG-silk scaffold showed compressive properties which were well within the midrange values of cancellous bone (2–12 MPa for compressive strength and 50–500 MPa for modulus[90,91]). Mechanical stability of a scaffold implant within the wound site is an important contributing factor to its regenerative capacity, and implants which replicate the mechanical environment of the target tissue by mimicking certain aspects of the native tissue architecture are likely to achieve improved reconstructive outcomes.[92] In the case of an osteochondral defect, the native articular joint surrounding the implant is expected to carry the majority of the applied load while the implant should undergo deformation that is consistent with loading on the neighbouring tissue.[93] The biphasic scaffold approximated the biomechanical behaviour of osteochondral tissue in compression, as the compliant cartilage phase could undergo large amounts of deformation while retaining the ability for shape recovery when hydrated, and the stiff bone phase could withstand large compressive stresses with minimal deformation. The biphasic scaffold therefore possessed favourable mechanical properties for promoting regeneration in a load-bearing osteochondral environment, as it could maintain structural integrity under large compressive stresses with no delamination or instability at the interface. Equally important was its biphasic mechanical behaviour corresponding to the cartilage and bone segments of osteochondral tissue, which could serve as differentiation cues as mesenchymal stem cells are known to respond to matrix stiffness.[94]

3.4 Cell attachment in the biphasic scaffold

Attachment and morphology of hMSCs cultured on the biphasic scaffold were assessed by SEM. At both 2 and 24 hours, attached cells were found in both phases of the biphasic scaffold and showed complete spreading on all surfaces (Fig. 6). The biphasic scaffold therefore facilitated the penetration of cells throughout its entire structure by allowing cell migration within and between phases. At 2 hours, cells in the cartilage phase formed many extended cell processes to contact the silk matrix, and many cells had already established connections with their neighbours (Fig. 6A). In the bone phase, cells were barely distinguishable as they were completely flattened on the surface of the SHG-silk scaffold (Fig. 6B). At 24 hours, cells in the cartilage phase became well-conformed to the surface of

the silk scaffold (Fig. 6C), while cells in the bone phase formed flattened sheets on the surface of the SHG-silk scaffold with webs of interconnected processes between adjacent cells (Fig. 6D). The SEM images showed that the biphasic scaffold was biocompatible and provided favourable substrates for cell attachment in its cartilage and bone phases, as well as a continuous interface which allowed cell migration and interaction between phases.

3.5 Histology and immunofluorescence to assess chondrogenic response in the biphasic scaffold

The chondrogenic response of hMSCs cultured in the cartilage phase of the biphasic scaffold over 21 days in chondrogenic medium was assessed by the deposition of cartilage-specific ECM, with the silk scaffold included as a separate group for comparison. Alcian blue staining was used to localise sulfated GAGs in the scaffolds as evidence of proteoglycan deposition (Fig. 7A – D). In both the silk scaffold and biphasic scaffold, cells infiltrated the interconnected pores of the silk matrix and positive staining was observed at depths well below the scaffold surface. The morphology of the cartilaginous matrix in the cartilage phase of the biphasic scaffold was similar to that in the silk scaffold, with a thin but dense outer layer of flattened cells followed by inner layers which were less dense but contained a rich matrix with large amounts of proteoglycans (Fig. 7A, B). At higher magnification, the elongated morphology of cells in the outer layer became evident, while cells in the inner layers exhibited a more rounded morphology (Fig. 7C, D). In both scaffold groups, the layered structure of the cartilaginous matrix with regional variations in cell morphology and matrix density matched well with the zoned architecture of native articular cartilage.[5] The formation of cartilage-specific ECM in the silk scaffold and biphasic scaffold was further confirmed by immunofluorescence staining of collagen type II as the major matrix component of hyaline cartilage (Fig. 7E – H). In both groups, abundant collagen type II deposition was observed around the outer edges (Fig. 7E, F) of the silk matrix as well as in the centre (Fig. 7G, H). The collagen appeared to have formed an extensive network which enveloped the cells and was interlaced with the pore structure of the silk construct. The collagen network observed in the silk scaffold and cartilage phase of the biphasic scaffold was reminiscent of the structural characteristics of articular cartilage, which consists mainly of an interconnected mesh of collagen type II fibrils within which the chondrocytes are embedded.[95] Collectively, the results indicated that the cartilage phase of the biphasic scaffold was able to facilitate the thorough infiltration, condensation and chondrogenic differentiation of hMSCs in an inductive environment. The consequent formation of cartilage-like tissue was evidenced by the deposition of proteoglycans and collagen type II as cartilage-specific ECM components, which were organised into a structured matrix that showed resemblance to the characteristics of mature hyaline cartilage. The silk scaffold achieved similar outcomes of chondrogenic induction when integrated into the biphasic scaffold and when cultured as a separate construct. The histological appearance of the resulting cartilaginous matrix was comparable to that observed in other studies when hMSCs were cultured over a few weeks under chondrogenic conditions in silk scaffolds formed via alternative fabrication routes.[66,68,71] The biphasic scaffold could hence be expected to support the formation of cartilaginous tissue during osteochondral regeneration corresponding to the distribution and structure of native hyaline cartilage.

3.6 Gene expression in the biphasic scaffold and its individual components

To investigate the differentiation response of hMSCs in the biphasic scaffold and the contribution of its individual components under *in vitro* conditions relevant to the osteochondral environment, gene expression of hMSCs cultured respectively in chondrogenic and osteogenic media on silk scaffolds, SHG ceramic scaffolds, SHG-silk scaffolds and biphasic scaffolds was measured over 21 days, and data for all genes tested were expressed as fold increase from undifferentiated cells at day 0. Sox-9, collagen type II, aggrecan and collagen type X were tested as markers of chondrogenic differentiation (Fig. 8), while Runx2, collagen type I, alkaline phosphatase and bone sialoprotein were tested as markers of osteogenic differentiation (Fig. 9).

When cultured in chondrogenic medium, differences in the expression levels of Sox-9 (Fig. 8A), collagen type II (Fig. 8C) and aggrecan (Fig. 8E) between groups displayed mostly similar trends. Differences between groups were not prominent at 4 days. At 14 and 21 days, expression levels of all three genes in the SHG ceramic and SHG-silk scaffolds were significantly higher compared to the biphasic scaffold, as well as compared to the silk scaffold in some cases particularly at 14 days. For each gene, the silk scaffold also showed significantly higher expression than the biphasic scaffold at either 14 or 21 days. Comparing the changes within each group over time, the SHG ceramic and SHG-silk scaffolds showed the same trend for Sox-9 (Fig. 8B), collagen type II (Fig. 8D) and aggrecan (Fig. 8F), where expression levels increased significantly from 4 to 14 days but dropped at 21 days. For the silk scaffold, Sox-9 expression remained constant over the culture period, while collagen type II and aggrecan expression increased until 14 days. For the biphasic scaffold, there were noticeable to significant increases in Sox-9, collagen type II and aggrecan expression compared to undifferentiated cells at 4 days, although expression levels remained relatively low over the culture period. Patterns of collagen type X expression were somewhat different from the other three genes when compared between and within groups. The SHG ceramic and SHG-silk scaffolds showed significantly higher expression of collagen type X compared to the silk scaffold at 4 days, and compared to both the silk scaffold and biphasic scaffold at 14 and 21 days (Fig. 8G). Expression levels in the silk scaffold were also significantly higher than in the biphasic scaffold at 14 days. Over time, collagen type X expression exhibited noticeable to significant increases in all groups except for the biphasic scaffold, which showed stable baseline expression at all time points (Fig. 8H).

The progression of chondrogenesis is a cellular event that occurs in multiple stages.[96] In a chondrogenic environment, pluripotent mesenchymal cells undergo condensation to form cell aggregates, which is an essential process in inducing their commitment to differentiation along the chondrocyte lineage and is marked by the expression of Sox-9.[97] This is followed by unidirectional proliferation, the production of cartilaginous matrix proteins and chondrocyte maturation. Collagen type II and aggrecan are two molecules essential to the structure and function of cartilage ECM. Collagen type II is the principle component of collagen fibrils that contributes to the tensile strength of articular cartilage, while aggrecan is the major proteoglycan by mass that contributes to compressive stiffness.[95] During skeletal growth by endochondral ossification, chondrocytes in the advancing growth plate undergo hypertrophy and are replaced by bone. The hypertrophic differentiation of chondrocytes is

marked by collagen type X expression, which results in matrix calcification and eventual death of the chondrocytes through apoptosis.[98] In light of the natural progression of events during chondrogenesis, collective analysis of the chondrogenic gene expression data revealed some interesting points. Based on the expression levels of Sox-9, collagen type II and aggrecan, it appeared that chondrogenic induction in the silk scaffold proceeded to a lesser extent than in the SHG ceramic and SHG-silk scaffolds at 14 days, but became comparable to the SHG-silk scaffold by 21 days. As the cartilage phase of the biphasic scaffold, the silk scaffold at least possessed similar ability as the SHG-silk scaffold of the bone phase in promoting the *in vitro* chondrogenesis of hMSCs particularly with increased time in culture. Concurrent analysis of collagen type X expression showed that significantly lower transcript levels of this gene were found in the silk scaffold compared to the SHG ceramic and SHG-silk scaffolds over the entire culture period. As a marker of chondrocyte hypertrophy, the high expression levels of collagen type X in the SHG ceramic and SHG-silk scaffolds suggested that the cells in these scaffold groups were proceeding towards osteogenesis following chondrogenic induction in a process that was reminiscent of endochondral ossification.[98] This explanation was plausible considering the high osteogenic capacity of the SHG ceramic and SHG-silk scaffolds,[59] and was supported by the observation that the chondrocyte phenotype was not maintained in these two groups as the expression levels of Sox-9, collagen type II and aggrecan dropped at 21 days compared to the previous time point. In contrast, the silk scaffold showed smaller increases in collagen type X expression over the culture period, which indicated the suppression of hypertrophic conversion following chondrogenic induction. The development and maintenance of the chondrocyte phenotype was therefore preferentially encouraged in the cartilage phase of the biphasic scaffold rather than the bone phase. Surprisingly, although the expression of chondrogenic markers increased over the culture period for its individual components, the biphasic scaffold showed baseline expression levels for all markers after the first time point. The hybrid structure of the biphasic scaffold might have provided increased surface area which needed to be populated by cells before the essential process of mesenchymal condensation could occur to drive chondrogenic differentiation.[99] The relatively low expression of chondrogenic markers in the biphasic scaffold pointed to the possible requirement for longer culture times[100] or pre-differentiation of progenitor cells[42] to achieve relevant chondrogenic outcomes *in vitro* with integrated scaffold designs.

When cultured in osteogenic medium, the scaffold groups showed time-related changes in the patterns of gene expression which were consistent with the temporal sequence of osteoblast development. Runx2 expression was similar between groups at 4 days but became significantly higher in the silk scaffold at 14 days compared to all other groups, and was also significantly lower in the biphasic scaffold compared to the SHG ceramic scaffold at 14 days and the SHG-silk scaffold at 21 days (Fig. 9A). Over the culture period, Runx2 expression remained stable in the silk scaffold, increased significantly in the biphasic scaffold only at 21 days, and displayed similar changes in the SHG ceramic and SHG-silk scaffolds where significantly higher transcript levels were detected at 4 days compared to undifferentiated cells followed by a significant drop and another significant increase at the subsequent time points (Fig. 9B). Collagen type I expression was significantly higher in the biphasic scaffold compared to the SHG-silk scaffold at 4 and 14 days, and compared to all

other groups at 21 days (Fig. 9C). Expression levels in the silk scaffold also significantly exceeded all other groups at 14 days. Comparison within each group showed mostly insignificant changes in collagen type I expression over time (Fig. 9D). Alkaline phosphatase expression showed no prominent differences between groups except at 21 days, where significantly higher levels were detected in both the biphasic scaffold and SHG-silk scaffold compared to the SHG ceramic scaffold (Fig. 9E). Increases in alkaline phosphatase expression within groups were significant at 4 days in the SHG ceramic and SHG-silk scaffolds compared to undifferentiated cells, and also at 21 days in both groups as well as in the biphasic scaffold (Fig. 9F). For bone sialoprotein, expression levels in the biphasic scaffold and SHG ceramic scaffold were significantly lower compared to the SHG-silk scaffold at 14 days, and compared to both the silk scaffold and SHG-silk scaffold at 21 days (Fig. 9G). All groups showed pronounced increases in bone sialoprotein expression over the culture period, particularly for the biphasic scaffold as significant changes were observed at all time points (Fig. 9H).

In an osteogenic environment, the commitment of pluripotent mesenchymal cells to differentiation along the osteoblast lineage is marked by the expression of Runx2.[101] This is followed by a temporal sequence of gene expression during development of the osteoblast phenotype which is defined by three distinct periods.[102,103] During the initial period of active proliferation, cell growth-related genes are expressed together with genes associated with the formation of bone ECM including collagen type I. Following the downregulation of proliferation, the period of matrix maturation occurs and is characterised by a peak in alkaline phosphatase expression, during which the composition and organisation of the ECM are modified in preparation for mineralisation. During the final period of matrix mineralisation, the genes of several proteins involved in mineral accumulation, including bone sialoprotein, are induced to maximal levels. Collective analysis of the osteogenic gene expression data indicated that the biphasic scaffold and its individual components could all support the progression of *in vitro* osteogenesis under inductive conditions. At the first time point, all groups showed elevated Runx2 expression of 1.5 to 2-fold compared to levels in undifferentiated cells, which evidenced equal ability to induce the commitment of hMSCs to osteogenic differentiation. In general for all of the osteogenic markers tested, mostly similar expression levels were observed between groups at the first time point and differences only became apparent at the later time points, further indicating that the different structural and material compositions in the biphasic scaffold and its individual components affected the rate of osteogenesis rather than its occurrence. The SHG-silk scaffold was shown to possess high osteogenic capacity which became particularly evident with increased time in culture, and greatly exceeded the SHG ceramic scaffold in the expression of markers for advanced osteoblast development and maturation, namely alkaline phosphatase and bone sialoprotein, at the later time points. The SHG-silk scaffold could therefore fulfill its role as the bone phase of the biphasic scaffold, due to a strong ability to encourage the commitment of progenitor cells to osteogenesis and the continuous progression of differentiation. However, although the biphasic scaffold contained the SHG-silk scaffold as one of its phases, it showed a slower rate of *in vitro* osteogenesis compared to the SHG-silk scaffold alone. This finding corroborated the gene expression patterns obtained when the scaffolds were cultured in chondrogenic medium, as the increased surface area offered by the hybrid structure of the

biphasic scaffold might have required longer culture times for cell population and aggregation before osteogenic differentiation could occur. As evidence of delayed progression in osteoblast development, the biphasic scaffold showed lower Runx2 expression, higher collagen type I expression, similar alkaline phosphatase expression and lower bone sialoprotein expression compared to the SHG-silk scaffold at the later time points. Based on the temporal sequence of osteogenic gene expression,[102] cells in the biphasic scaffold appeared to have only reached the end of the proliferative period and onset of matrix maturation by 21 days and strong induction of genes for matrix mineralisation had not yet occurred at this time point. Nevertheless, as it supported consistent increases in the expression of markers for advanced osteogenesis over the culture period, the biphasic scaffold was competent for promoting the osteogenic differentiation of hMSCs in an inductive environment, and could be expected to match the enhanced osteogenic behaviour observed in the SHG-silk scaffold with longer culture times. Interestingly, despite having a soft and elastic matrix that was less likely to encourage osteogenic differentiation, the silk scaffold frequently showed enhanced expression of both early and late osteogenic markers compared to the other groups at the later time points. This was likely the result of lower porosity and smaller pore sizes in the silk scaffold, which had known effects of inducing cell aggregation and osteogenic differentiation *in vitro*[78] and possibly superseded the influence of matrix stiffness.

Several inferences could be made from the *in vitro* differentiation behaviour of hMSCs cultured in the biphasic scaffold and its individual components under both chondrogenic and osteogenic conditions. When tested in parallel as separate groups, scaffolds constituting the cartilage and bone phases of the biphasic scaffold respectively induced chondrogenic and osteogenic differentiation, suggesting that the biphasic scaffold had the capacity to support stratified regenerative responses in its integrated phases corresponding to the anatomical segments of osteochondral tissue. However, the induction of chondrogenic or osteogenic behaviour was not necessarily exclusive to the matching phase in the biphasic scaffold, and the biphasic scaffold itself achieved similar levels of osteogenesis compared to its individual phases but lower levels of chondrogenesis. This might be explained by the fact that the differentiation responses of hMSCs *in vitro* depended mainly on the type of inductive medium used rather than structural or material composition of the scaffold, as shown in a study which attempted *in vitro* chondrogenic and osteogenic induction of hMSCs in an integrated scaffold which had already reached clinical translation.[100] A very different situation would be expected *in vivo* as cell differentiation would result from a complex mixture of physical, mechanical and biological cues present in the osteochondral environment.[89] The role of an integrated scaffold in mimicking the structural organisation and functionality of native ECM in order to promote appropriate tissue growth therefore becomes more imperative in this setting.[11] With the stratified properties offered by its integrated phases, the biphasic scaffold could be expected to fulfil this role and provide an optimal environment to guide cell ingrowth and differentiation towards *in vivo* osteochondral regeneration.

The experiments performed in this study established the key physical, mechanical and *in vitro* characteristics of a novel biphasic scaffold concept, and also provided insights into the

mechanisms governing observed scaffold behaviour in the context of osteochondral regeneration. Nevertheless, some limitations of the *in vitro* work remain to be addressed in future experiments. Firstly, large errors were sometimes observed in the gene expression results mainly for the silk scaffold and biphasic scaffold under both chondrogenic and osteogenic conditions. This was possibly the result of diffusional limitations imposed by static *in vitro* culture, as the silk scaffold and biphasic scaffold contained a silk matrix with lower porosity and smaller pore sizes than the SHG ceramic scaffold and SHG-silk scaffold, which were more likely to experience restrictions in the transport of oxygen and nutrients in the deeper layers of the scaffold. This might have restricted the extent of cell growth and differentiation in the silk scaffold and biphasic scaffold which in turn led to larger variations in the levels of gene expression. More consistent results can be produced in future studies by employing bioreactor cultivation to introduce a dynamic culture environment. Secondly, cell activity in the interface region of the biphasic scaffold was not specifically investigated. During scaffold-based osteochondral regeneration, complex cell interactions are likely to be present in the interface and might have an important role in mediating appropriate differentiation responses in the cartilage and bone compartments. The consequent generation of a biomimetic interface is important to the mechanical and biological function of the osteochondral scaffold and warrants further investigation in future studies. Lastly, this study only characterised the *in vitro* behaviour of hMSCs cultured in the biphasic scaffold as a whole compared to its individual components under different inductive conditions (chondrogenic or osteogenic), which could not account for the potential interactions between different cell populations in the cartilage and bone segments of osteochondral tissue or the potential contributions of an inductive gradient of bioactive factors to the outcome of cell differentiation. To more accurately mimic the biochemical and cellular gradient found in the *in vivo* osteochondral environment, future studies will consider the co-culture of two or more distinct cell populations in the cartilage and bone phases of the biphasic scaffold, use of both differentiated and undifferentiated cell sources, induction of differentiation or maintenance of differentiated phenotype using a mixture or gradient of chondrogenic and osteogenic media, and combinations of these strategies.

4. Conclusion

The design of a biphasic scaffold with stratified properties tailored for the regeneration of osteochondral tissue was developed and optimised in this study, and its characteristics were systematically investigated in light of the diverse and complex sets of requirements for the restoration of both articular cartilage and subchondral bone. Results indicated that the rational combination of silk fibroin with a bioactive ceramic via optimised fabrication processes could produce a unique construct that circumvented the common problems of integrated scaffold designs. Specifically, the biphasic scaffold possessed a stratified structure composed of distinct cartilage and bone phases which were well-integrated at a continuous interface, contained a bone phase that was well-matched to cancellous bone in structure and mechanical properties, and provided a gradient of physical, mechanical and biological cues to direct the differentiation of mesenchymal stem cells corresponding to the osteochondral anatomy. By featuring simple and reproducible fabrication methods and the potential to be applied in absence of supplementation with cells or bioactive molecules, the

biphasic scaffold also satisfied practical requirements which represented important but often overlooked factors in the efficient translation of scaffold-based approaches for clinical use. Future work will focus on *in vivo* integration and build towards applications in tissue engineering to improve on the insufficiency of current treatment modalities for the management and reconstruction of osteochondral defects.

Supplementary Material

Refer to Web version on PubMed Central for supplementary material.

Acknowledgements

The authors gratefully acknowledge the financial support of the Australian National Health and Medical Research Council, the U.S. National Institutes of Health (P41 EB002520, R01 DE106525), the Rebecca Cooper Foundation, the Australian Postgraduate Award and the Vice-Chancellor's Research Scholarship.

References

1. Redman SN, Oldfield SF, Archer CW. Eur. Cells Mater. 2005; 9:23–32.
2. Mithoefer K, McAdams T, Williams RJ, Kreuz PC, Mandelbaum BR. Am. J. Sports Med. 2009; 37:2053–2063. [PubMed: 19251676]
3. Jakob RP, Franz T, Gautier E, Mainil-Varlet P. Clin. Orthop. Relat. Res. 2002; 401:170–184. [PubMed: 12151894]
4. Harris JD, Siston RA, Brophy RH, Lattermann C, Carey JL, Flanigan DC. Osteoarthritis Cartilage. 2011; 19:779–791. [PubMed: 21333744]
5. Alford JW, Cole BJ. Am. J. Sports Med. 2005; 33:295–306. [PubMed: 15701618]
6. Jeon JE, Vaquette C, Klein TJ, Hutmacher DW. Anat. Rec. 2014; 297:26–35.
7. Keeney M, Pandit A. Tissue Eng., Part B. 2009; 15:55–73.
8. Mano JF, Reis RL. J. Tissue Eng. Regener. Med. 2007; 1:261–273.
9. Martin I, Miot S, Barbero A, Jakob M, Wendt D. J. Biomech. 2007; 40:750–765. [PubMed: 16730354]
10. Nooeaid P, Salih V, Beier JP, Boccaccini AR. J. Cell. Mol. Med. 2012; 16:2247–2270. [PubMed: 22452848]
11. O'Shea TM, Miao X. Tissue Eng., Part B. 2008; 14:447–464.
12. Mayr HO, Klehm J, Schwan S, Hube R, Südkamp NP, Niemeyer P, Salzmann G, von Eisenhardt-Rothe R, Heilmann A, Bohner M, Bernstein A. Acta Biomater. 2013; 9:4845–4855. [PubMed: 22885682]
13. Bernstein A, Niemeyer P, Salzmann G, Südkamp NP, Hube R, Klehm J, Menzel M, von Eisenhart-Rothe R, Bohner M, Görz L, Mayr HO. Acta Biomater. 2013; 9:7490–7505. [PubMed: 23528497]
14. Chang C-H, Kuo T-F, Lin C-C, Chou C-H, Chen K-H, Lin F-H, Liu H-C. Biomaterials. 2006; 27:1876–1888. [PubMed: 16278014]
15. Coburn JM, Gibson M, Monagle S, Patterson Z, Elisseeff JH. Proc. Natl. Acad. Sci. U. S. A. 2012; 109:10012–10017. [PubMed: 22665791]
16. Guo X, Wang C, Duan C, Descamps M, Zhao Q, Dong L, Lü S, Anselme K, Lu J, Song YQ. Tissue Eng. 2004; 10:1830–1840. [PubMed: 15684691]
17. Guo X, Wang C, Zhang Y, Xia R, Hu M, Duan C, Zhao Q, Dong L, Lu J, Song YQ. Tissue Eng. 2004; 10:1818–1829. [PubMed: 15684690]
18. Jung MR, Shim IK, Chung HJ, Lee HR, Park YJ, Lee MC, Yang YI, Do SH, Lee SJ. J. Controlled Release. 2012; 162:485–491.
19. Wang W, Li B, Yang J, Xin L, Li Y, Yin H, Qi Y, Jiang Y, Ouyang H, Gao C. Biomaterials. 2010; 31:8964–8973. [PubMed: 20822812]

20. Kandel RA, Grynpas M, Pilliar R, Lee J, Wang J, Waldman S, Zalzal P, Hurtig M. Biomaterials. 2006; 27:4120–4131. [PubMed: 16564568]
21. Shimomura K, Moriguchi Y, Ando W, Nansai R, Fujie H, Hart DA, Gobbi A, Kita K, Horibe S, Shino K, Yoshikawa H, Nakamura N. Tissue Eng., Part A. 2014; 20:2291–2304. [PubMed: 24655056]
22. Tuli R, Nandi S, Li WJ, Tuli S, Huang X, Manner PA, Laquerriere P, Nöth U, Hall DJ, Tuan RS. Tissue Eng. 2004; 10:1169–1179. [PubMed: 15363173]
23. Wang X, Grogan SP, Rieser F, Winkelmann V, Maquet V, La Berge M, Mainil-Varlet P. Biomaterials. 2004; 25:3681–3688. [PubMed: 15020143]
24. Chen J, Chen H, Li P, Diao H, Zhu S, Dong L, Wang R, Guo T, Zhao J, Zhang J. Biomaterials. 2011; 32:4793–4805. [PubMed: 21489619]
25. Cui W, Wang Q, Chen G, Zhou S, Chang Q, Zuo Q, Ren K, Fan W. J. Biosci. Bioeng. 2011; 111:493–500. [PubMed: 21208828]
26. Marquass B, Somerson JS, Hepp P, Aigner T, Schwan S, Bader A, Josten C, Zscharnack M, Schulz RM. J. Orthop. Res. 2010; 28:1586–1599. [PubMed: 20973061]
27. Miot S, Brehm W, Dickinson S, Sims T, Wixmerten A, Longinotti C, Hollander AP, Mainil-Varlet P, Martin I. Eur. Cells Mater. 2012; 23:222–236.
28. Pei M, He F, Boyce BM, Kish VL. Osteoarthritis Cartilage. 2009; 17:714–722. [PubMed: 19128988]
29. Schaefer D, Martin I, Jundt G, Seidel J, Heberer M, Grodzinsky A, Bergin I, Vunjak-Novakovic G, Freed LE. Arthritis Rheum. 2002; 46:2524–2534. [PubMed: 12355501]
30. Shao X, Goh JCH, Hutmacher DW, Lee EH, Zigang G. Tissue Eng. 2006; 12:1539–1551. [PubMed: 16846350]
31. Alhadlaq A, Elisseeff J, Hong L, Williams C, Caplan A, Sharma B, Kopher R, Tomkoria S, Lennon D, Lopez A, Mao J. Ann. Biomed. Eng. 2004; 32:911–923. [PubMed: 15298429]
32. Lam J, Lu S, Meretoja VV, Tabata Y, Mikos AG, Kasper FK. Acta Biomater. 2014; 10:1112–1123. [PubMed: 24300948]
33. Sheehy EJ, Vinardell T, Buckley CT, Kelly DJ. Acta Biomater. 2013; 9:5484–5492. [PubMed: 23159563]
34. Dormer NH, Singh M, Zhao L, Mohan N, Berkland CJ, Detamore MS. J. Biomed. Mater. Res., Part A. 2012; 100A:162–170.
35. Erisken C, Kalyon DM, Wang H, Örnek-Ballanco C, Xu J. Tissue Eng., Part A. 2010; 17:1239–1252. [PubMed: 21189068]
36. Mohan N, Dormer NH, Caldwell KL, Key VH, Berkland CJ, Detamore MS. Tissue Eng., Part A. 2011; 17:2845–2855. [PubMed: 21815822]
37. Re'em T, Witte F, Willbold E, Ruvinov E, Cohen S. Acta Biomater. 2012; 8:3283–3293. [PubMed: 22617742]
38. Chen G, Sato T, Tanaka J, Tateishi T. Mater. Sci. Eng., C. 2006; 26:118–123.
39. Da H, Jia SJ, Meng GL, Cheng JH, Zhou W, Xiong Z, Mu YJ, Liu J. PLoS One. 2013; 8:e54838. [PubMed: 23382984]
40. Deng T, Lv J, Pang J, Liu B, Ke J. J. Tissue Eng. Regener. Med. 2014; 8:546–556.
41. Duan P, Pan Z, Cao L, He Y, Wang H, Qu Z, Dong J, Ding J. J. Biomed. Mater. Res., Part A. 2014; 102:180–192.
42. Galperin A, Oldinski RA, Florczyk SJ, Bryers JD, Zhang M, Ratner BD. Adv. Healthcare Mater. 2013; 2:872–883.
43. Giannoni P, Lazzarini E, Ceseracciu L, Barone AC, Quarto R, Scaglione S. J. Tissue Eng. Regener. Med. 2012
44. Jiang C-C, Chiang H, Liao C-J, Lin Y-J, Kuo T-F, Shieh C-S, Huang Y-Y, Tuan RS. J. Orthop. Res. 2007; 25:1277–1290. [PubMed: 17576624]
45. Jiang J, Tang A, Ateshian GA, Guo XE, Hung CT, Lu HH. Ann. Biomed. Eng. 2010; 38:2183–2196. [PubMed: 20411332]
46. Tampieri A, Sandri M, Landi E, Pressato D, Francioli S, Quarto R, Martin I. Biomaterials. 2008; 29:3539–3546. [PubMed: 18538387]

47. Lien S-M, Chien C-H, Huang T-J. Mater. Sci. Eng., C. 2009; 29:315–321.
48. Oliveira JM, Rodrigues MT, Silva SS, Malafaya PB, Gomes ME, Viegas CA, Dias IR, Azevedo JT, Mano JF, Reis RL. Biomaterials. 2006; 27:6123–6137. [PubMed: 16945410]
49. Zhang S, Chen L, Jiang Y, Cai Y, Xu G, Tong T, Zhang W, Wang L, Ji J, Shi P, Ouyang HW. Acta Biomater. 2013; 9:7236–7247. [PubMed: 23567945]
50. Li JJ, Kaplan DL, Zreiqat H. J. Mater. Chem. B. 2014; 2:7272–7306.
51. Kon E, Delcogliano M, Filardo G, Pressato D, Busacca M, Grigolo B, Desando G, Marcacci M. Injury. 2010; 41:693–701. [PubMed: 20035935]
52. Kon E, Delcogliano M, Filardo G, Busacca M, Di Martino A, Marcacci M. Am. J. Sports Med. 2011; 39:1180–1190. [PubMed: 21310939]
53. Filardo G, Kon E, Di Martino A, Busacca M, Altadonna G, Marcacci M. Am. J. Sports Med. 2013; 41:1786–1793. [PubMed: 23761684]
54. Delcogliano M, de Caro F, Scaravella E, Ziveri G, De Biase C, Marotta D, Marenghi P, Delcogliano A. Knee Surg. Sports Traumatol. Arthrosc. 2014; 22:1260–1269. [PubMed: 24146051]
55. Carmont MR, Carey-Smith R, Saithna A, Dhillon M, Thompson P, Spalding T. Arthroscopy. 2009; 25:810–814. [PubMed: 19560648]
56. Barber FA, Dockery WD. Arthroscopy. 2011; 27:60–64. [PubMed: 20952149]
57. Dhollander AAM, Liekens K, Almqvist KF, Verdonk R, Lambrecht S, Elewaut D, Verbruggen G, Verdonk PCM. Arthroscopy. 2012; 28:225–233. [PubMed: 22014478]
58. Kim UJ, Park J, Kim HJ, Wada M, Kaplan DL. Biomaterials. 2005; 26:2775–2785. [PubMed: 15585282]
59. Roohani-Esfahani SI, Dunstan CR, Li JJ, Lu Z, Davies B, Pearce S, Field J, Williams R, Zreiqat H. Acta Biomater. 2013; 9:7014–7024. [PubMed: 23467040]
60. Tamada Y. Biomacromolecules. 2005; 6:3100–3106. [PubMed: 16283733]
61. de Vries-van Melle ML, Narcisi R, Kops N, Koevoet WJLM, Bos PK, Murphy JM, Verhaar JAN, van der Kraan PM, van Osch GJVM. Tissue Eng., Part A. 2013; 20:23–33. [PubMed: 23980750]
62. Gomoll A, Madry H, Knutsen G, van Dijk N, Seil R, Brittberg M, Kon E. Knee Surg. Sports Traumatol. Arthrosc. 2010; 18:434–447. [PubMed: 20130833]
63. Li JJ, Gil ES, Hayden RS, Li C, Roohani-Esfahani S-I, Kaplan DL, Zreiqat H. Biomacromolecules. 2013; 14:2179–2188. [PubMed: 23745709]
64. Raghunath J, Rollo J, Sales KM, Butler PE, Seifalian AM. Biotechnol. Appl. Biochem. 2007; 46:73–84. [PubMed: 17227284]
65. Vepari C, Kaplan DL. Prog. Polym. Sci. 2007; 32:991–1007. [PubMed: 19543442]
66. Hofmann S, Knecht S, Langer R, Kaplan DL, Vunjak-Novakovic G, Merkle HP, Meinel L. Tissue Eng. 2006; 12:2729–2738. [PubMed: 17518642]
67. Makaya K, Terada S, Ohgo K, Asakura T. J. Biosci. Bioeng. 2009; 108:68–75. [PubMed: 19577196]
68. Meinel L, Hofmann S, Karageorgiou V, Zichner L, Langer R, Kaplan D, Vunjak-Novakovic G. Biotechnol. Bioeng. 2004; 88:379–391. [PubMed: 15486944]
69. Wang Y, Bella E, Lee CSD, Migliaresi C, Pelcastre L, Schwartz Z, Boyan BD, Motta A. Biomaterials. 2010; 31:4672–4681. [PubMed: 20303584]
70. Wang Y, Blasioli DJ, Kim HJ, Kim HS, Kaplan DL. Biomaterials. 2006; 27:4434–4442. [PubMed: 16677707]
71. Wang Y, Kim UJ, Blasioli DJ, Kim HJ, Kaplan DL. Biomaterials. 2005; 26:7082–7094. [PubMed: 15985292]
72. Wang Y, Rudym DD, Walsh A, Abrahamsen L, Kim HJ, Kim HS, Kirker-Head C, Kaplan DL. Biomaterials. 2008; 29:3415–3428. [PubMed: 18502501]
73. Chen QZ, Thompson ID, Boccaccini AR. Biomaterials. 2006; 27:2414–2425. [PubMed: 16336997]
74. Kundu SC, Kundu B, Talukdar S, Bano S, Nayak S, Kundu J, Mandal BB, Bhardwaj N, Botlagunta M, Dash BC, Acharya C, Ghosh AK. Biopolymers. 2012; 97:455–467. [PubMed: 22241173]

75. Kawakami M, Tomita N, Shimada Y, Yamamoto K, Tamada Y, Kachi N, Suguro T. Bio-Med. Mater. Eng. 2011; 21:53–61.
76. Nazarov R, Jin HJ, Kaplan DL. Biomacromolecules. 2004; 5:718–726. [PubMed: 15132652]
77. Karageorgiou V, Kaplan D. Biomaterials. 2005; 26:5474–5491. [PubMed: 15860204]
78. Sundelacruz S, Kaplan DL. Semin. Cell Dev. Biol. 2009; 20:646–655. [PubMed: 19508851]
79. Santos MI, Reis RL. Macromol. Biosci. 2010; 10:12–27. [PubMed: 19688722]
80. Jin QM, Takita H, Kohgo T, Atsumi K, Itoh H, Kuboki Y. J. Biomed. Mater. Res. 2000; 52:841–851.
81. Kuboki Y, Jin Q, Takita H. J. Bone Jt. Surg. 2001; 83:S105–S115.
82. Kuboki Y, Jin Q, Kikuchi M, Mamood J, Takita H. Connect. Tissue Res. 2002; 43:529–534. [PubMed: 12489210]
83. Pins GD, Christiansen DL, Patel R, Silver FH. Biophys. J. 1997; 73:2164–2172. [PubMed: 9336212]
84. Engelberg I, Kohn J. Biomaterials. 1991; 12:292–304. [PubMed: 1649646]
85. Gobin AS, Froude VE, Mathur AB. J. Biomed. Mater. Res., Part A. 2005; 74A:465–473.
86. Gibson LJ. J. Biomech. 2005; 38:377–399. [PubMed: 15652536]
87. Levingstone TJ, Matsiko A, Dickson GR, O'Brien FJ, Gleeson JP. Acta Biomater. 2014; 10:1996–2004. [PubMed: 24418437]
88. Laasanen MS, Töyräs J, Korhonen RK, Rieppo J, Saarakkala S, Nieminen MT, Hirvonen J, Jurvelin JS. Biorheology. 2003; 40:133–140. [PubMed: 12454397]
89. Castro N, Hacking SA, Zhang L. Ann. Biomed. Eng. 2012; 40:1628–1640. [PubMed: 22677924]
90. Rezwan K, Chen QZ, Blaker JJ, Boccaccini AR. Biomaterials. 2006; 27:3413–3431. [PubMed: 16504284]
91. Hutmacher DW, Schantz JT, Lam CXF, Tan KC, Lim TC. J. Tissue Eng. Regener. Med. 2007; 1:245–260.
92. Guilak F, Butler DL, Goldstein SA, Baaijens FPT. J. Biomech. 2014; 47:1933–1940. [PubMed: 24818797]
93. Harley BA, Lynn AK, Wissner-Gross Z, Bonfield W, Yannas IV, Gibson LJ. J. Biomed. Mater. Res., Part A. 2010; 92A:1078–1093.
94. Kelly DJ, Jacobs CR. Birth Defects Res., Part C. 2010; 90:75–85.
95. Poole AR, Kojima T, Yasuda T, Mwale F, Kobayashi M, Laverty S. Clin. Orthop. Relat. Res. 2001; 391:S26–S33. [PubMed: 11603710]
96. Vinatier C, Mrugala D, Jorgensen C, Guicheux J, Noël D. Trends Biotechnol. 2009; 27:307–314. [PubMed: 19329205]
97. Akiyama H. Mod. Rheumatol. 2008; 18:213–219. [PubMed: 18351289]
98. Magne D, Vinatier C, Julien M, Weiss P, Guicheux J. Trends Mol. Med. 2005; 11:519–526. [PubMed: 16213191]
99. Johnstone B, Hering TM, Caplan AI, Goldberg VM, Yoo JU. Exp. Cell Res. 1998; 238:265–272. [PubMed: 9457080]
100. Manferdini C, Cavallo C, Grigolo B, Fiorini M, Nicoletti A, Gabusi E, Zini N, Pressato D, Facchini A, Lisignoli G. J. Tissue Eng. Regener. Med. 2013
101. Komori T. Cell Tissue Res. 2010; 339:189–195. [PubMed: 19649655]
102. Lian JB, Stein GS. Iowa Orthop. J. 1995; 15:118–140. [PubMed: 7634023]
103. Owen TA, Aronow M, Shalhoub V, Barone LM, Wilming L, Tassinari MS, Kennedy MB, Pockwinse S, Lian JB, Stein GS. J. Cell. Physiol. 1990; 143:420–430. [PubMed: 1694181]

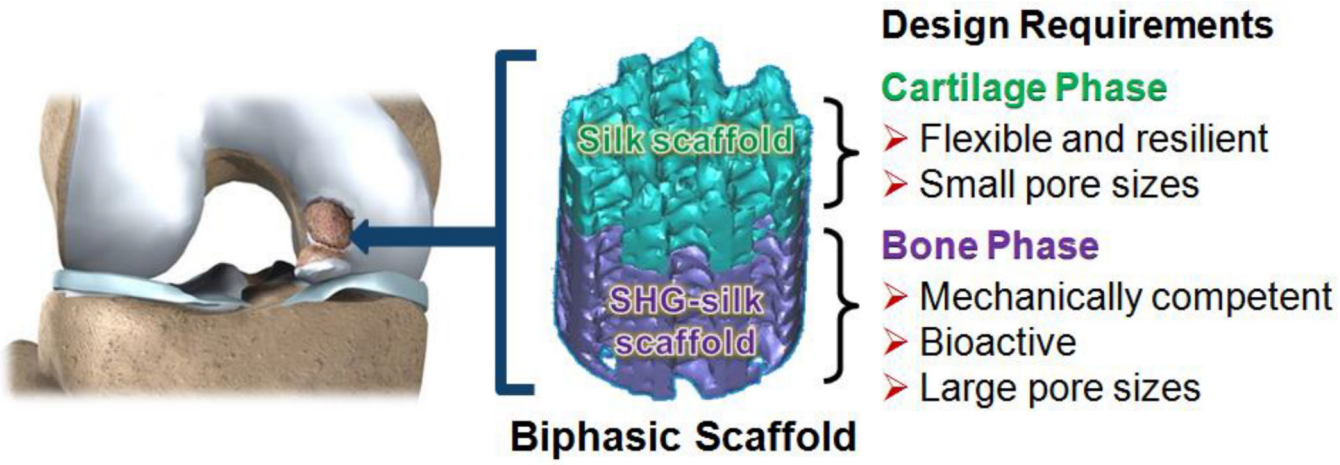

Fig. 1.
Design concept of the biphasic scaffold for osteochondral regeneration.

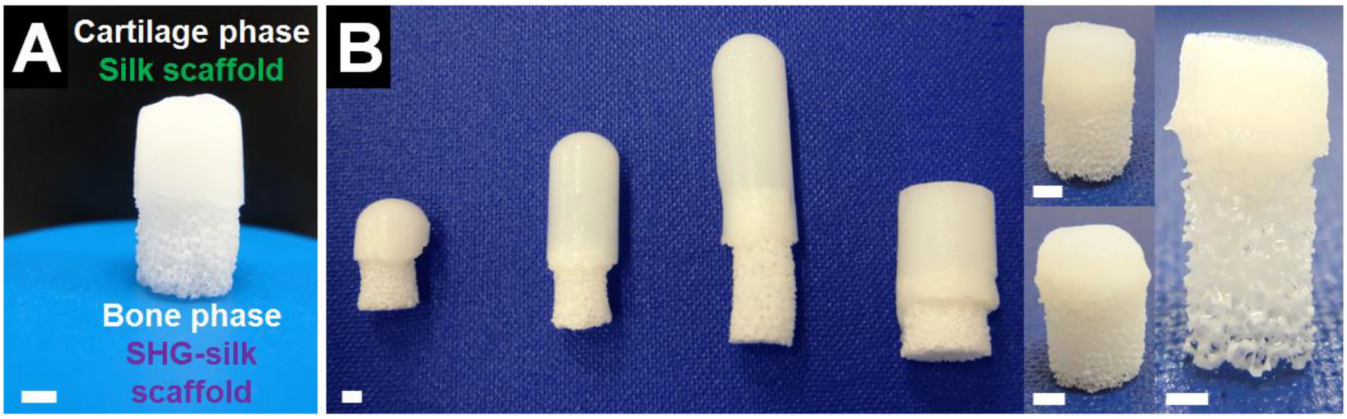

Fig. 2.

(A) Biphasic scaffold with two distinct and well-integrated phases formed via an optimised method of fabrication, and **(B)** range of biphasic scaffolds which could be easily and reproducibly fabricated with customised dimensions. Scale bar = 2mm.

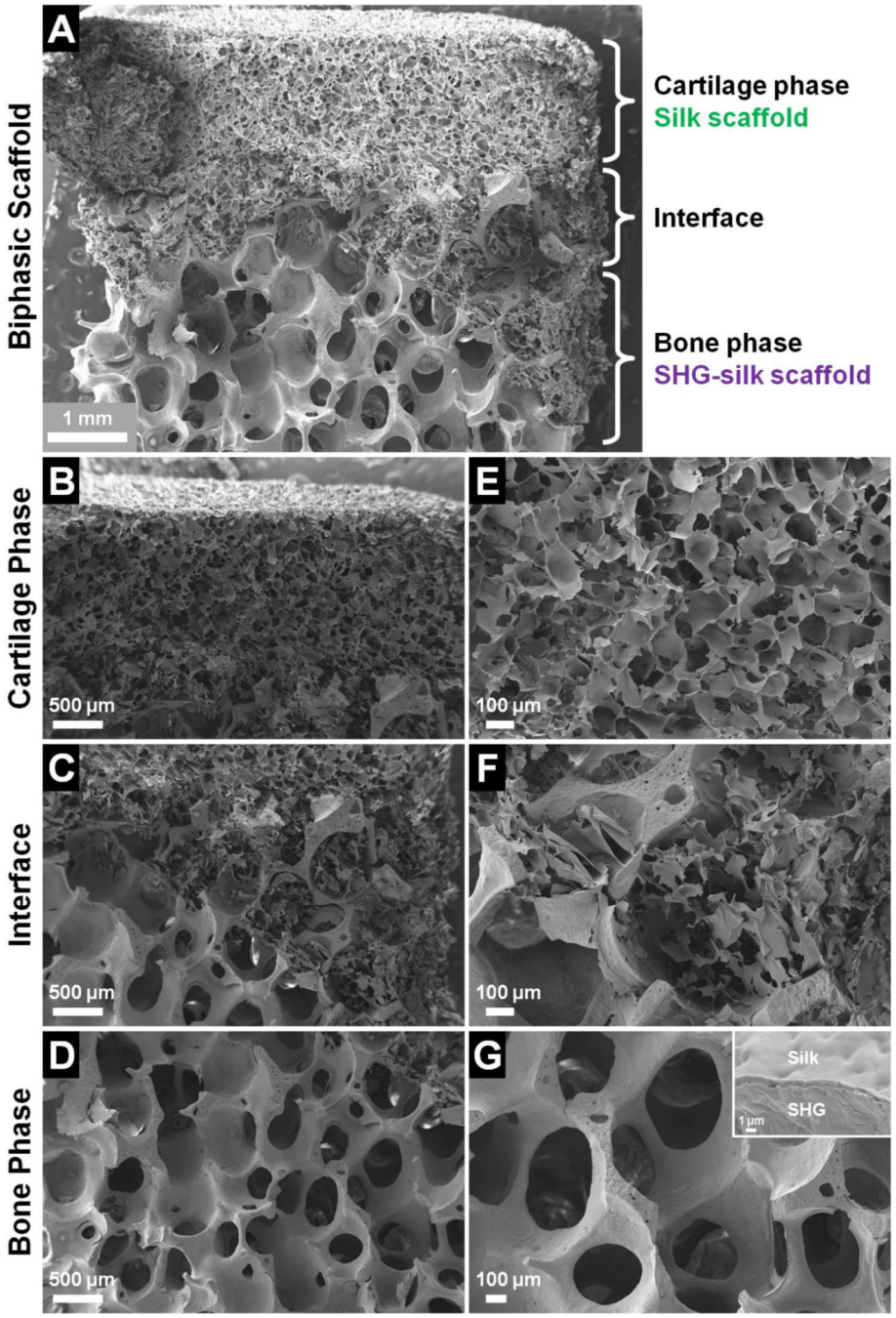

Fig. 3.

Microscopic morphology of the biphasic scaffold, showing **(A)** complete scaffold, **(B)** cartilage phase, **(C)** interface region, **(D)** bone phase, and **(E–G)** structural features at higher magnifications.

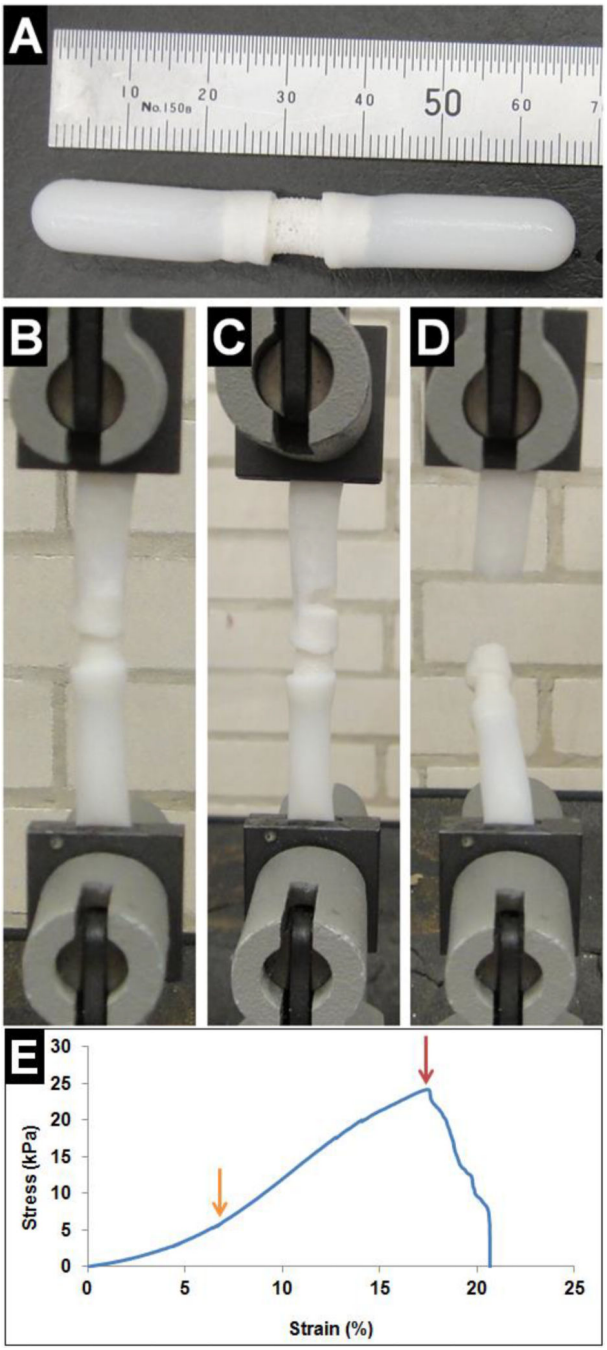

Fig. 4.

Interfacial bonding strength of the biphasic scaffold was determined in tension. **(A)** Modified biphasic scaffold used for testing, **(B–D)** interface behaviour in tension, and **(E)** the corresponding stress-strain curve. The meanings of the arrows are explained in the text.

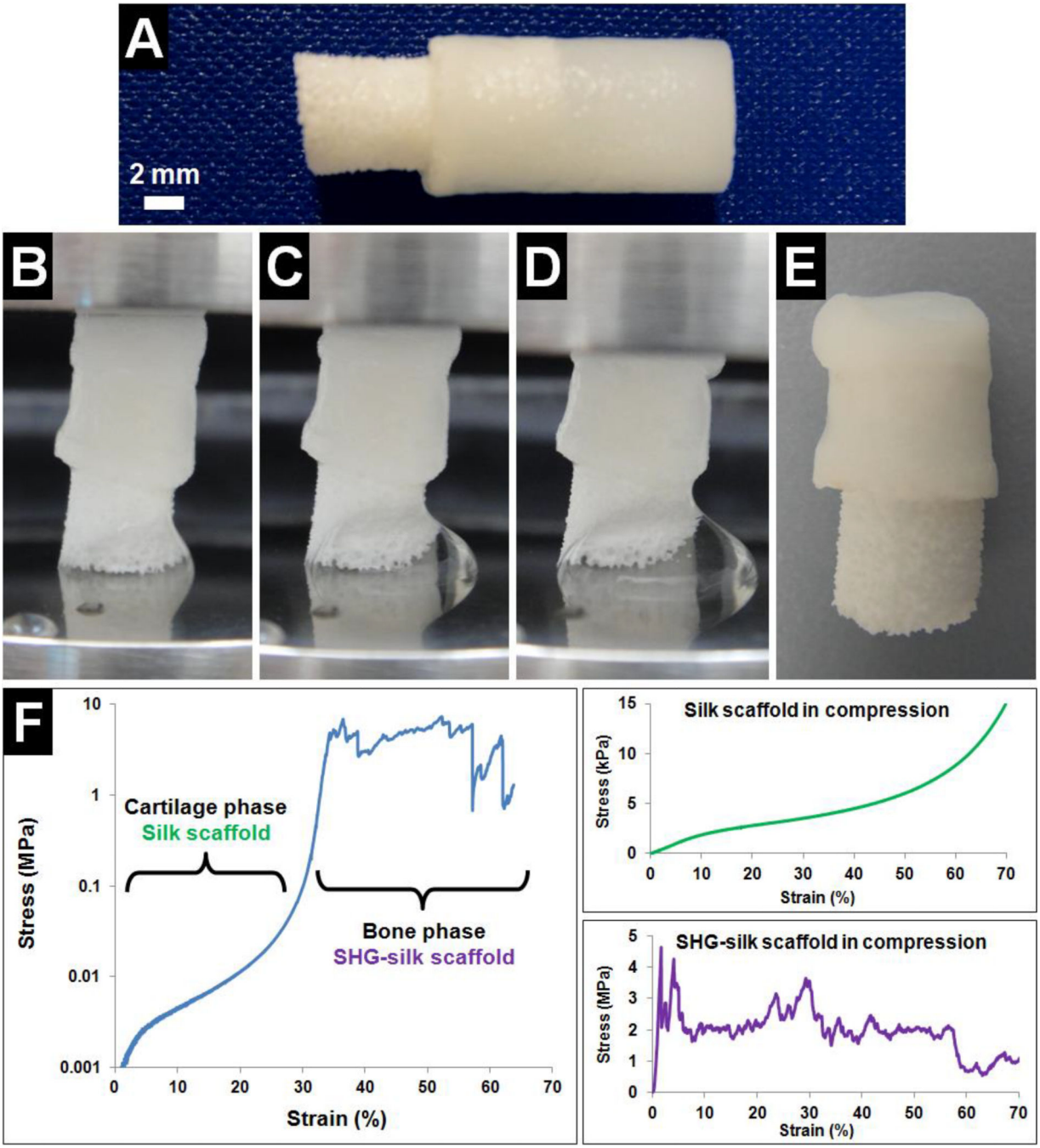

Fig. 5.

Mechanical behaviour of the biphasic scaffold was determined in compression. **(A)** Biphasic scaffold used for testing, **(B–D)** deformation behaviour in compression, **(E)** sample retrieved after testing to failure, and **(F)** the corresponding stress-strain curve (together with stress-strain curves of the silk scaffold and SHG-silk scaffold tested as independent constructs for comparison).

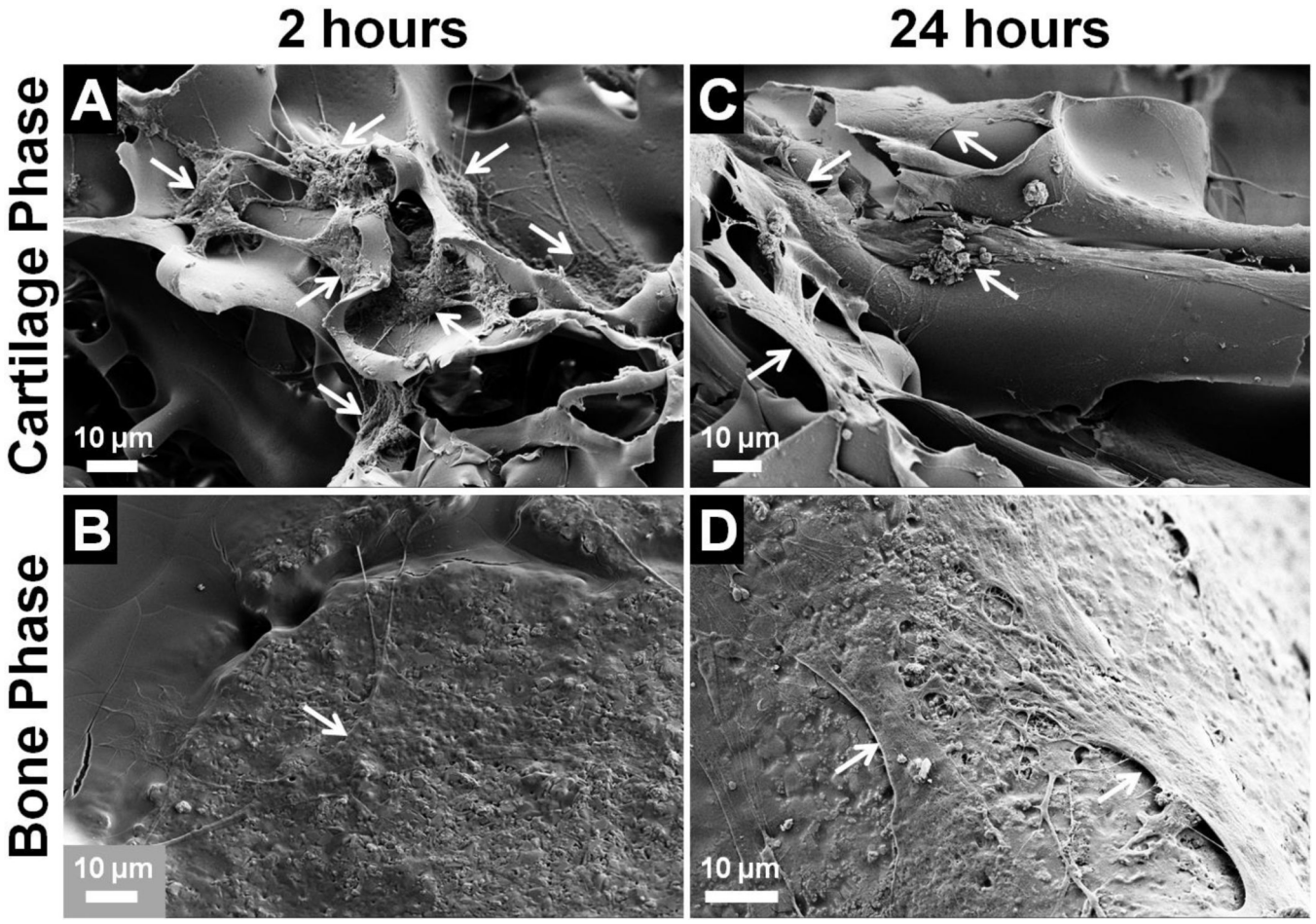

Fig. 6.

Attachment and morphology of hMSCs cultured on the biphasic scaffold after **(A, B)** 2 hours and **(C, D)** 24 hours. Arrows indicate attached cells on the scaffold surface.

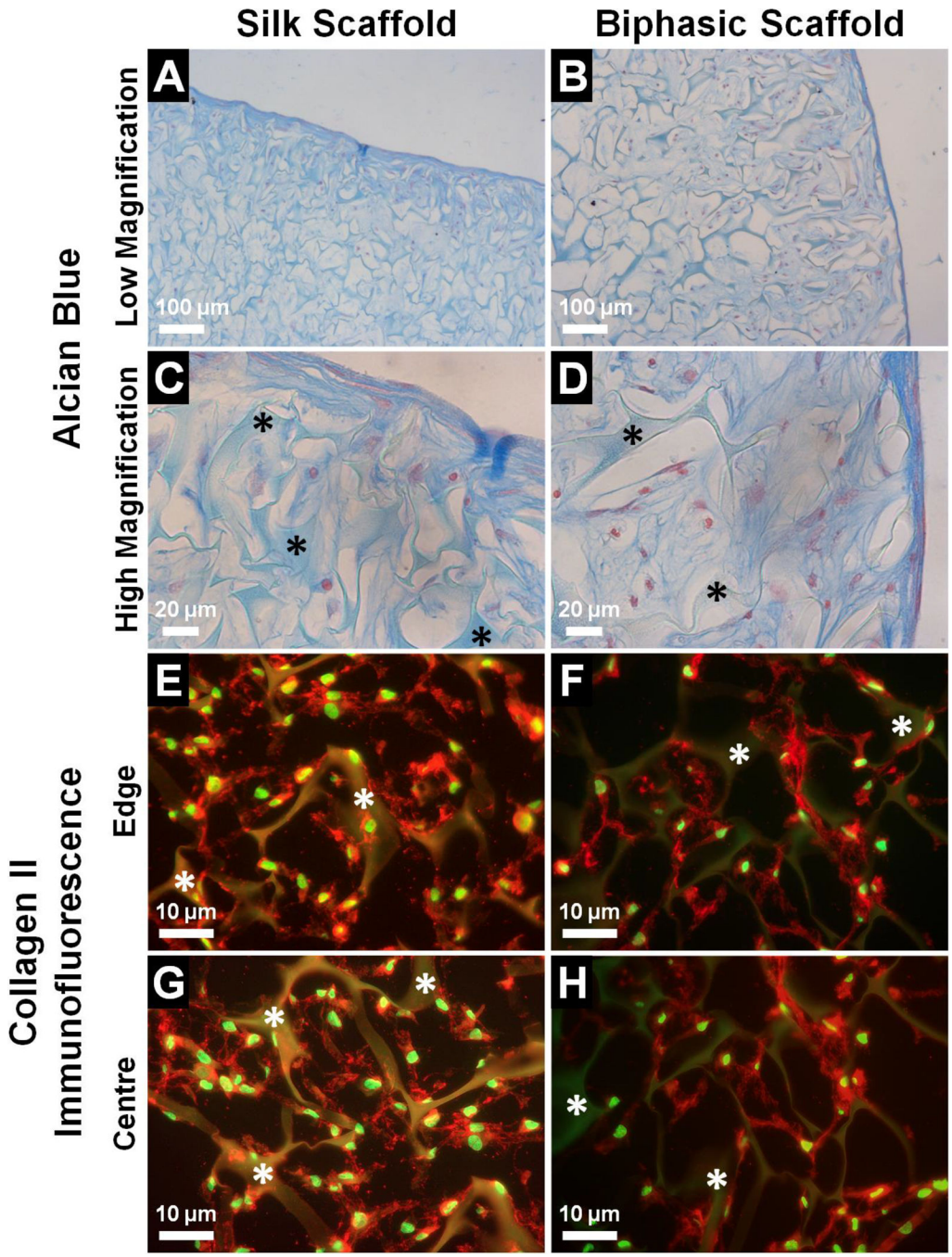

Fig. 7.

Deposition of cartilage-specific ECM by hMSCs cultured in the cartilage phase of the biphasic scaffold compared to the silk scaffold after 21 days in chondrogenic medium, as assessed by **(A–D)** Alcian blue staining for proteoglycans (blue = sulfated GAGs, red = cell nuclei), and **(E–H)** collagen type II immunofluorescence (red = collagen type II, green = cell nuclei). Asterisks indicate the silk matrix.

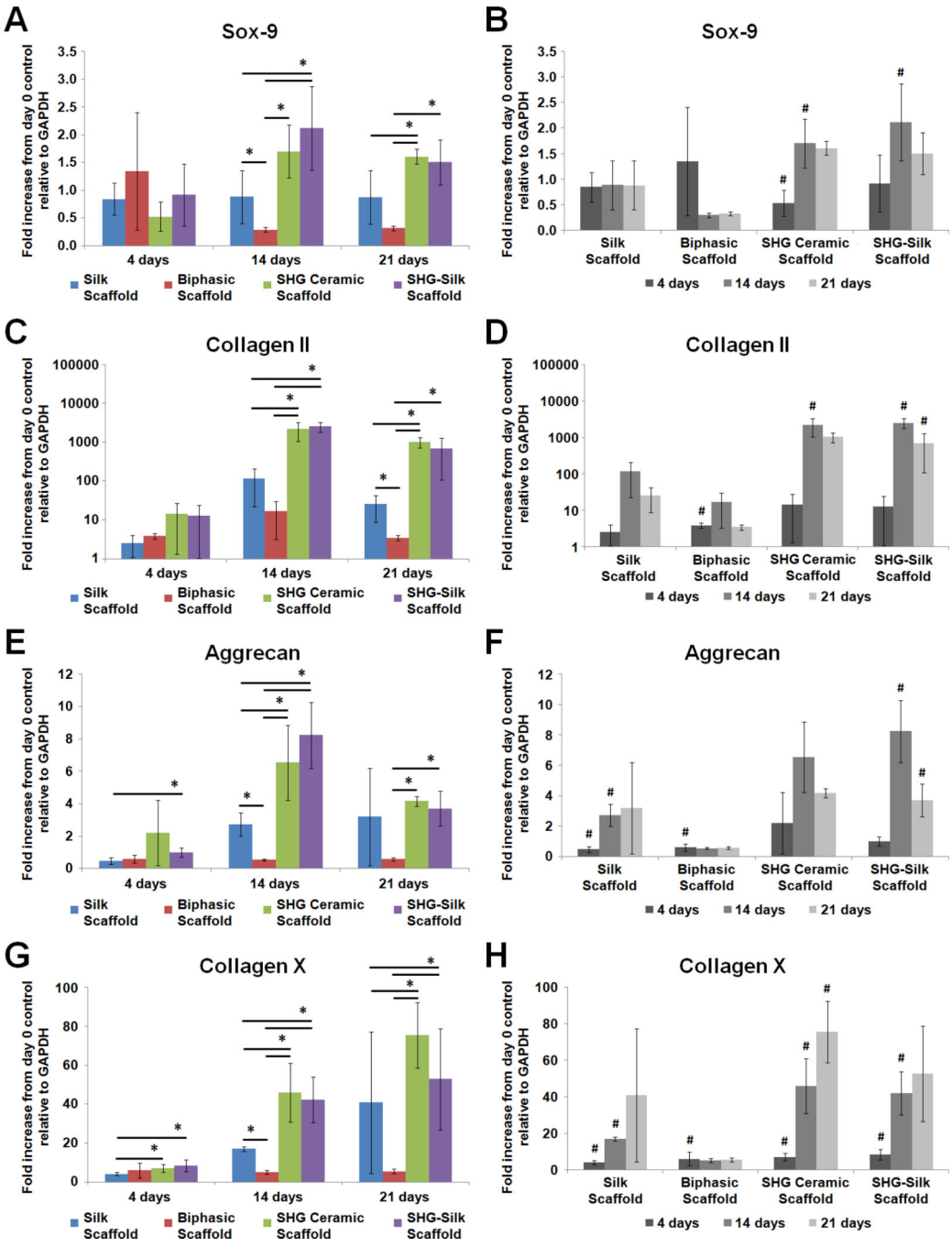

Fig. 8.

Gene expression of hMSCs cultured on silk scaffolds, SHG ceramic scaffolds, SHG-silk scaffolds and biphasic scaffolds in chondrogenic medium over 21 days, expressed as fold increase from undifferentiated cells at day 0. **(A, B)** Sox-9, **(C, D)** collagen type II, **(E, F)** aggrecan, and **(G, H)** collagen type X. (A, C, E, G) show differences in expression levels between groups (*$p < 0.05$ between groups) while (B, D, F, H) show changes in expression levels within each group over the culture period ($^{\#}p < 0.05$ within the same group compared to previous time point).

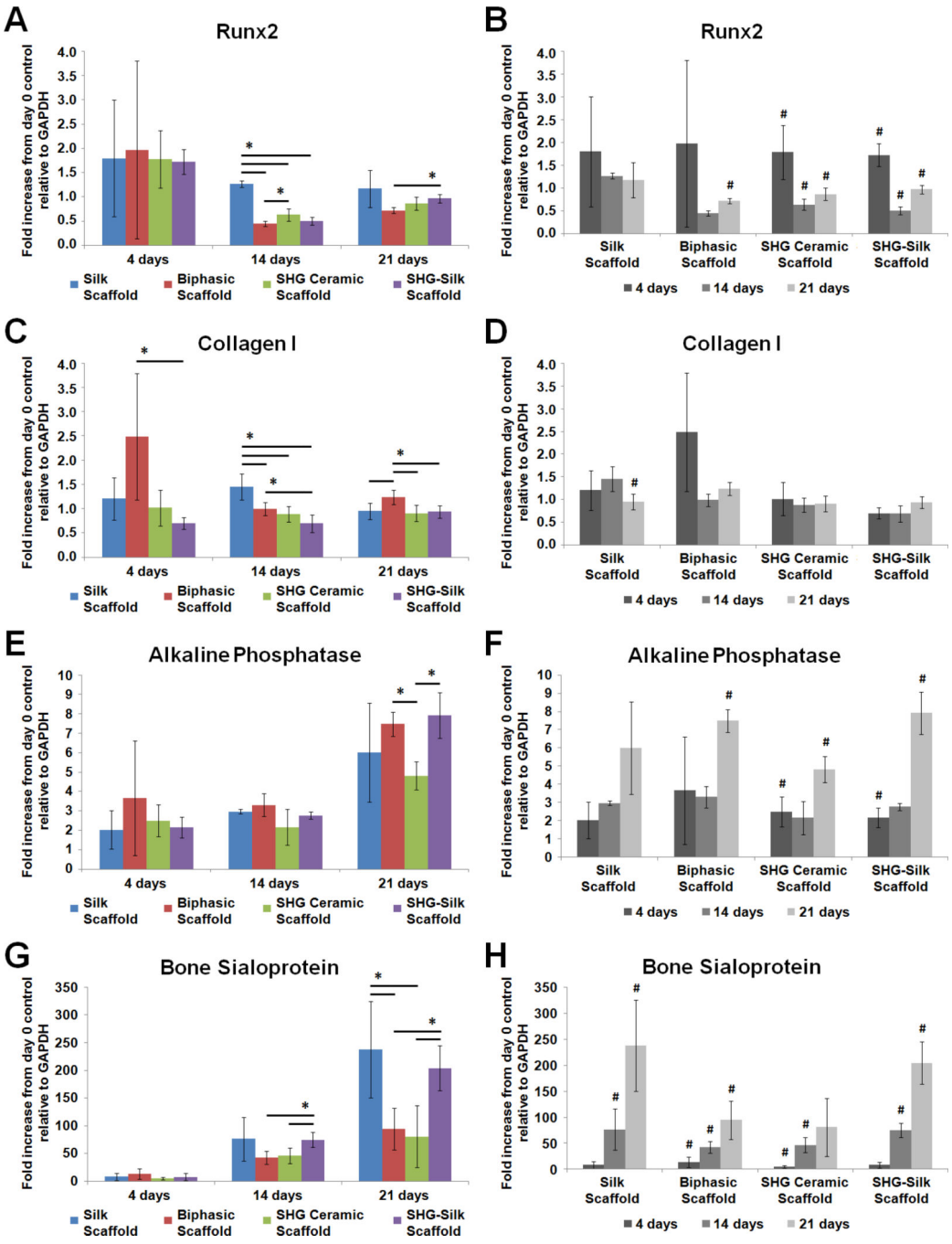

Fig. 9.

Gene expression of hMSCs cultured on silk scaffolds, SHG ceramic scaffolds, SHG-silk scaffolds and biphasic scaffolds in osteogenic medium over 21 days, expressed as fold increase from undifferentiated cells at day 0. **(A, B)** Runx2, **(C, D)** collagen type I, **(E, F)** alkaline phosphatase, and **(G, H)** bone sialoprotein. (A, C, E, G) show differences in expression levels between groups (*$p < 0.05$ between groups) while (B, D, F, H) show

changes in expression levels within each group over the culture period ($^{\#}p < 0.05$ within the same group compared to previous time point).

Table 1

Compressive properties of the biphasic scaffold presented as values for each of its two phases.

Biphasic Scaffold Phases	Compressive Strength	Compressive Modulus
Cartilage phase Silk scaffold	2.7 ± 0.4 kPa	139 ± 29 kPa
Bone phase SHG-silk scaffold	7.2 ± 2.5 MPa	266 ± 63 MPa